

1 **A review of microplastics aggregation in aquatic environment:**
2 **Influence factors, analytical methods, and environmental**
3 **implications**

4 Xinjie Wang ^a, Nanthi Bolan ^b, Daniel C.W. Tsang ^c, Sarkar Binoy ^d, Lauren Bradney ^b,

5 Yang Li ^{a,*}

6 *^a Key Laboratory of Water and Sediment Sciences of Ministry of Education, State Key*
7 *Laboratory of Water Environment Simulation, School of Environment, Beijing Normal*
8 *University, Beijing 100875, PR China*

9 *^b Faculty of Science, University of Newcastle, Callaghan, NSW, Australia*

10 *^c Department of Civil and Environmental Engineering, The Hong Kong Polytechnic*
11 *University, Hung Hom, Kowloon, Hong Kong, China*

12 *^d Lancaster Environment Centre, Lancaster University, Lancaster, LA1 4YQ, United*
13 *Kingdom*

14

15

16 Corresponding Author

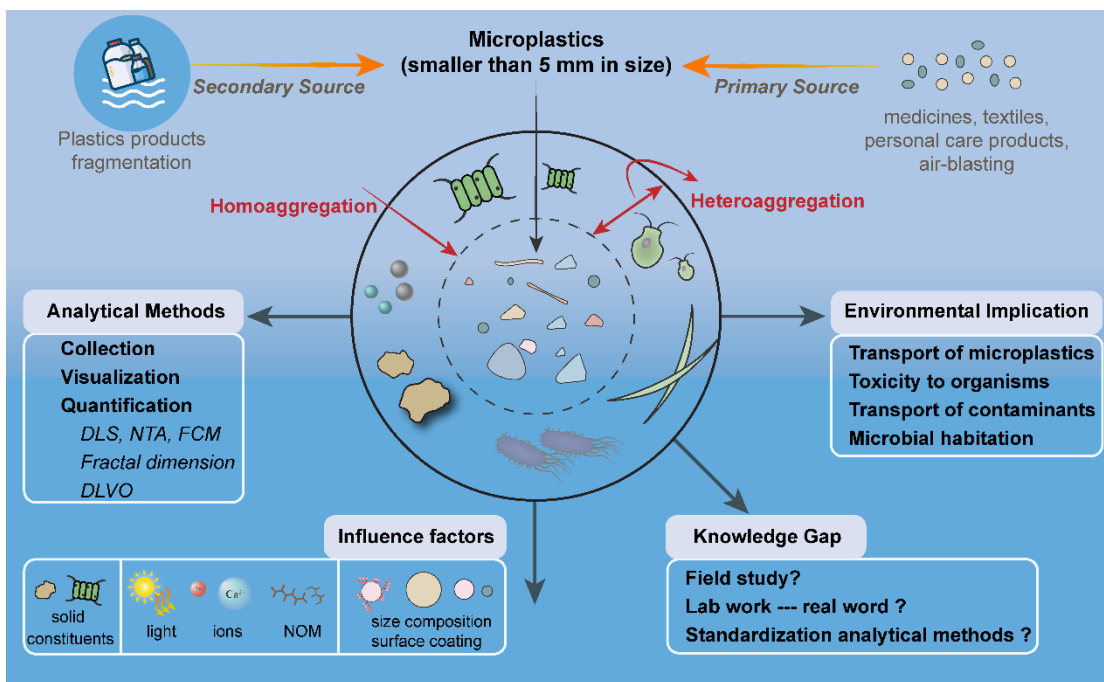
17 *Phone: +86-10-5880-7612; e-mail: liyang_bnu@bnu.edu.cn (Y.L.).

18 **Highlights**

- 19 • The aggregation of MPs in real aquatic environment is far from fully understood.
- 20 • Sampling and analyzing methods for studying MP aggregation were summarized.
- 21 • Influence factors and environmental implications of MP aggregation were reviewed.
- 22 • MP aggregation in the field and their temporal stability deserve extensive research.
- 23 • Laboratory studies should use MPs representing those in real aquatic environment.

24

25 **Graphical abstract**



26

27

28 **Abstract:** A large amount of plastic waste released into natural waters and their
29 demonstrated toxicity have made the transformation of microplastics (MPs; < 5 mm) and
30 nanoplastics (NPs; < 100 nm) an emerging environmental concern. Aggregation is one of
31 the most important environmental behaviors of MPs, especially in aquatic environments,
32 which determines the mobility, distribution and bioavailability of MPs. In this paper, the
33 sources and inputs of MPs in aquatic environments were first summarized followed by the
34 analytical methods for investigating MP aggregation, including the sampling, visualization,
35 and quantification procedures of MP' particle sizes. We critically evaluated the sampling
36 methods that still remains a methodological gap. Identification and quantification of MPs
37 were mostly carried out by visual, spectroscopic and spectrometric techniques, and
38 modeling analysis. Important factors affecting MP aggregation in natural waters and
39 environmental implications of the aggregation process were also reviewed. Finally,
40 recommendations for future research were discussed, including (1) conducting more field
41 studies; (2) using MPs in laboratory works representing those in the environment; and (3)
42 standardizing methods of identification and quantification. The review gives a
43 comprehensive overview of current knowledge for MP aggregation in natural waters,
44 identifies knowledge gaps, and provides suggestions for future research.

45 **Keywords:** Microbead, Stability, Detection methods, Microbial habitation, Contaminant
46 vector

47 **Abbreviations**

48 nanoplastics (NPs)
49 microplastics (MPs)
50 polystyrene (PS)

51 polyethylene (PE)
52 polypropylene (PP)
53 polyvinyl chloride (PVC)
54 poly(methyl methacrylate) (PMMA)
55 amino-modified PS NPs (PSNPs-NH₂)
56 carboxyl-modified PS NPs (PSNPs-COOH)
57 ultraviolet (UV)
58 humic acid (HA)
59 laser diffraction (LD)
60 fractal dimensions (D_f)
61 flow cytometry (FCM)
62 attachment efficiency (α)
63 hydrodynamic diameter (D_h)
64 exopolymeric substances (EPS)
65 field flow fractionation (FFF)
66 dynamic light scattering (DLS)
67 atomic force microscopy (AFM)
68 dissolved organic matter (DOM)
69 extended DLVO-theory (eDLVO)
70 nanoparticle tracking analysis (NTA)
71 scanning electron microscopy (SEM)
72 energy dispersive spectroscopy (EDS)
73 wastewater treatment plants (WWTPs)
74 hydrodynamic chromatography (HDC)
75 transmission electron microscopy (TEM)
76 critical coagulation concentration (CCC)

77 Derjaguin-Landau-Verwey-Overbeek (DLVO)
78 Fourier-transform infrared spectroscopy (FTIR)
79 asymmetrical flow field-flow fractionation (AF4)

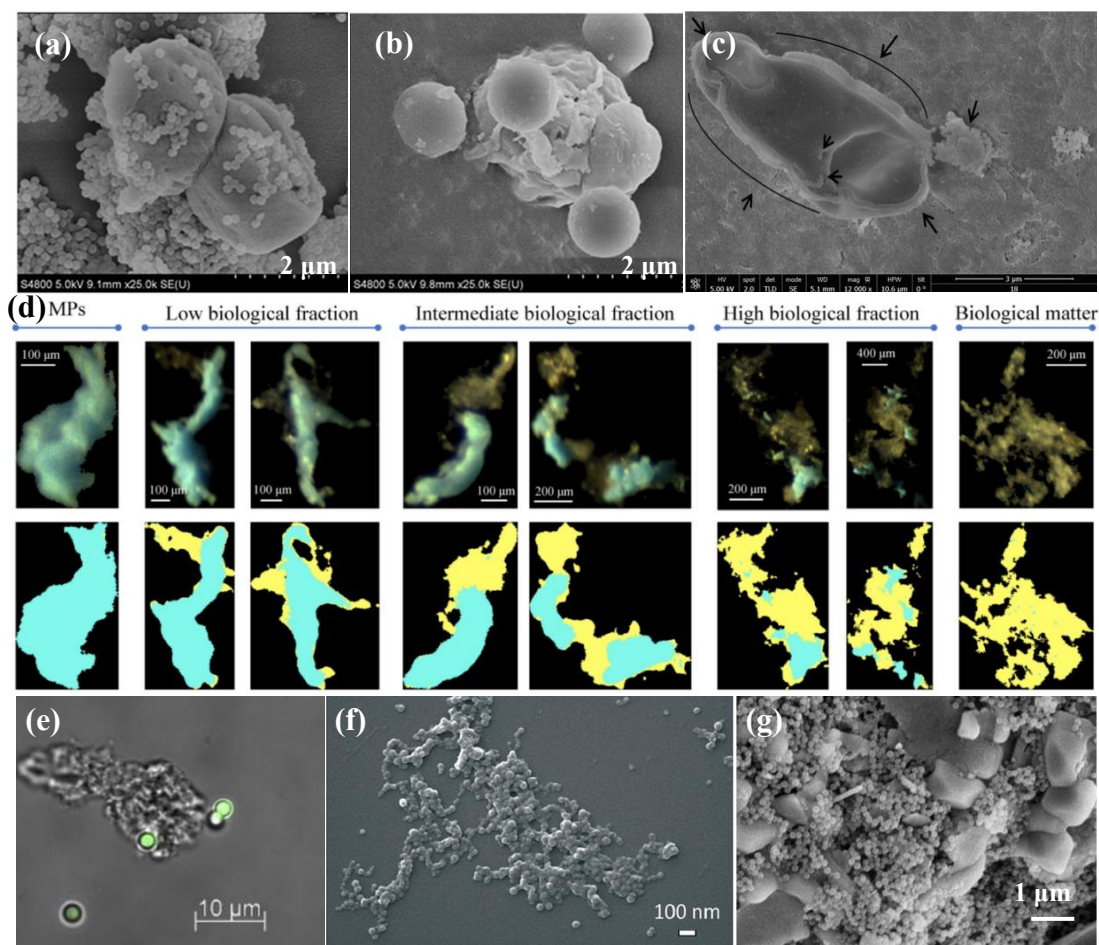
80

81 **1. Introduction**

82 Microplastics (MPs) and nanoplastics (NPs) are defined as plastic particles with
83 diameters < 5 mm and < 100 nm, respectively (Feng et al., 2020). Scientists agree that the
84 pollution of MPs in marine and freshwater environments have potential adverse impacts
85 on aquatic organisms, marine ecosystems and even human health (Castelvetto et al., 2020;
86 Wang and Wang, 2018). Regulators and researchers currently assess the environment risk
87 of MPs relying upon their ecotoxicity tests and environmental fate modeling (Karbalaie et
88 al., 2018). Aggregation of MPs is an important physical-chemical process dominating the
89 transport behavior and overall fate of MPs in aquatic environments (Alimi et al., 2018).
90 Recent investigations on MP aggregation have focused on simulated natural waters in
91 laboratory, while the process in complex heterogeneous media or in natural waters is
92 largely unknown (Singh et al., 2019). Adequate experimental protocols and environmental
93 fate models are needed to develop for theoretically understanding and quantifying the
94 aggregation process of the MP pollutants (Praetorius et al., 2020).

95 Aggregation involves the transport of two particles toward each other to collide,
96 followed by attachment (Zhang, 2014). This can occur between the same type of MPs
97 (homoaggregation) or different types of particles (heteroaggregation) (Alimi et al., 2018).
98 Compared with the homoaggregation of MPs, the heteroaggregation of MPs with other
99 solid constituents such as natural minerals and seaweeds is more prone to occur in natural
100 waters driving the floating, sedimentation, and resuspension processes of MPs (Long et al.,

101 2017; Oriekhova and Stoll, 2018; Singh et al., 2019). The organism-associated aggregation
102 of MPs/NPs have been widely reported, as shown in **Fig.1** a-e. Plastic surfaces commonly
103 contain hydrophobic functional groups that facilitate the adsorption of dissolved organic
104 matter (DOM) and organisms, especially algae and bacteria (Zhang et al., 2020). Microbial
105 habitation and biofilm formation are common on MP surface in natural waters (Harrison et
106 al., 2018). Apart from organism-associated MP aggregates, organic matter (e.g., alginate)
107 (**Fig. 1** f), layered clay minerals (e.g., suspended sediment (**Fig. 1** g), Fe_2O_3), and
108 nanoparticles also could aggregate with MPs (Li et al., 2020). Because of the inherently
109 higher system complexity, studies on heteroaggregation of MPs are still scarce (Oriekhova
110 and Stoll, 2018).



111

112 **Fig. 1.** Major types of aggregates formed by microplastics (MPs)/nanoplastics (NPs). (a)
 113 0.1 mm polystyrene MPs (PS MPs) aggregate with *Chlorella pyrenoidosa* (Mao et al.,
 114 2018); (b) 1.0 mm PS MPs aggregate with *Chlorella pyrenoidosa* (Mao et al., 2018); (c)
 115 100 nm PS NPs aggregate with marine microalgae *Phaeodactylum tricornutum* (Sendra et
 116 al., 2019); (d) Samples of microbial-associated MP aggregates obtained by optical
 117 measurement of cell colonization (Bäbler et al., 2020); (e) Micrograph of PS MPs (green)
 118 aggregate with bacteria (Long et al., 2017); (f) SEM image of NPs in the presence of
 119 alginate (Oriekhova and Stoll, 2018); (g) SEM image of suspended sediments (100-500
 120 μm) associated PS NPs heteroaggregates (Li et al., 2019). Figures are adapted from
 121 references mentioned above with permission.

122 The aggregation of MPs in aquatic environments has mainly been studied in
 123 laboratories with simulated water samples due to the limitation of collection and detection
 124 techniques in studying in the field (Oriekhova and Stoll, 2018). Recently, a number of
 125 review papers summarized the sampling methods of natural water samples to investigate

126 the mass and distribution of MPs in water columns (Cutroneo et al., 2020). However, some
127 sampling methods such as the density separation method using electrolyte might change
128 the particle size of MPs (Cutroneo et al., 2020; Prata et al., 2019). Therefore, these methods
129 are not quite applicable for investigating the stability of MPs in water. During
130 characterizing the size distribution of MPs using light-scattering methods, the detection
131 might be hampered by the low concentration of MPs in environmental samples or by the
132 complexity of real environmental media (Praetorius et al., 2020). Only a few studies exist
133 to investigate the aggregation of plastic particles at the micro- and nanometer size fractions
134 in complex matrices, because of the practical and fundamental challenges for isolation and
135 analysis of particulate plastics smaller than 100 μm (Gigault et al., 2016; Nguyen et al.,
136 2019). Therefore, the limitations and advantages of various sampling and detection
137 methods have been compared in this review to facilitate the investigation of MP stability
138 in real waters, which has not been well summarized before.

139 The distribution and toxicity of MPs has been the focus of numerous recent works
140 (Wu et al., 2019b). Only a few review papers have paid attention to the research progresses
141 on MP aggregation in water, which are of particular concern, because their changed particle
142 sizes might influence their own transformation, co-transport with other contaminants, and
143 the toxicity to organisms (Yang et al., 2018). It has been demonstrated that the toxicity of
144 PS NPs was higher than that of PS MPs toward *Brachionus koreanus*, *Paracyclops nana*,
145 *Daphnia magna*, and *Tigriopus japonicus* (Choi et al., 2019). Till now, studies were
146 primarily focused on the aggregation of spherical polystyrene (PS) MPs with various
147 particle-specific properties (e.g., size and surface coating) (Dong et al., 2018; Romero-
148 Cano et al., 2001; Yu et al., 2019). There remain little data on the aggregation of MPs with

149 other compositions or shapes. In addition, the water chemical conditions play dominant
150 roles in MP aggregation, but often the effect of a single water chemical condition was taken
151 into consideration in laboratory experiments (Singh et al., 2019). Few reviews discussed
152 the key factors governing MP aggregation and the impact of MP aggregation on the
153 transport of contaminants (Alimi et al., 2018; Gigault et al., 2018; Huffer et al., 2017). Thus,
154 it is necessary to conduct a systematic and comprehensive literature review summarizing
155 the quantitative information and modelling of MP aggregation and environmental impacts
156 of MP aggregation.

157 This paper provides a critical overview of the recent progress in investigating the
158 aggregation of MPs in aquatic environment, especially in the last three years. First, we
159 review the sources and inputs of MPs in aquatic environments. Next, we critically delineate
160 the sampling, visualization and quantification methods for studying MP aggregation. In
161 addition, the main influencing factors of MP aggregation including their own
162 physicochemical properties and environmental conditions are summarized. The potential
163 environmental implications of MP aggregation in water, particularly in the toxicity to
164 organisms and microbial habitation are discussed. Finally, the current gaps in knowledge
165 and suggestions regarding future research on MP aggregation are discussed. The main
166 objectives of this review paper are to: (1) obtain a clear understanding of MP aggregation;
167 (2) propose to establish standardized sampling programs and field studies for investigating
168 MP aggregation; and (3) facilitate a better understanding of potential environmental risks
169 related to MPs aggregation.

170 **2. Sources and inputs of microplastics in aquatic environments**

171 MPs are a ubiquitous water contaminant, present in lakes, oceans, and even arctic ice

172 (Zobkov and Esiukova, 2018). Once in the aquatic environment, wind, run-off, and ocean
173 currents aid in their transport, allowing them to travel well beyond their source. Many of
174 the behaviors (e.g., degradation, weathering, and adsorption of contaminants) associated
175 with MPs are influenced by their pathways of transport and surrounding environment
176 (Chamas et al., 2020). One important behaviour is the aggregation process of MPs upon
177 entering the aquatic environment (Li et al., 2018). To fully understand this behavior and
178 associated interactions, the sources and inputs of MPs first need to be discussed.

179 **2.1 Primary sources of microplastics in aquatic environments**

180 Primary MPs are the manufactured plastic particles with diameters < 5 mm that
181 perform a specific function within or enhance the requirements of a product (Lei et al.,
182 2017). Examples of primary MPs include those used for or found within personal care
183 products, air-blasting, medicines, and textiles (Fendall and Sewell, 2009). Of all the
184 primary MPs, cosmetic microbeads have received the most attention (Guerranti et al.,
185 2019). Natural exfoliating agents such as crushed fruit stones were originally used within
186 facial scrubs until the cosmetic industry found that exfoliation could be achieved by adding
187 small plastic fragments or beads with low cost (Fendall and Sewell, 2009). Unfortunately,
188 facial scrubs are ‘rinsed-off’, and consequently, wastewater treatment plants (WWTPs)
189 became a sink for MPs (Murphy et al., 2016). The deluge of research condemning
190 microbeads has resulted in their slow phase-out. Although the Netherlands was the first
191 country to state their intent to ban cosmetic microbeads by 2016, it was within the United
192 States that the first national legislation, the *Microbead-Free Waters Act* of 2015, was
193 passed (United States Congress, 2015; Xanthos and Walker, 2017). Air-blasting has also
194 been reported as a source of primary MPs when a less abrasive material is required for

195 cleaning or paint stripping (Auta et al., 2017). MPs and polymeric film coatings also aid
196 medical drug delivery by acting as a vector and increasing control (Cole et al., 2011).
197 Therefore, the medical industry is also a source of plastic particles (Chamas et al., 2020).
198 Finally, some MPs arise from textile and clothing fibers (Galafassi et al., 2019). However,
199 their classification is somewhat of a grey area as they can be either primary or secondary
200 MPs. The fibers are a result of fabric shredding during manufacture (primary), machine
201 washing of clothes, or after the clothes are discarded to landfill (secondary) (Cole et al.,
202 2011).

203 **2.2 Secondary sources of microplastics in aquatic environments**

204 Alternatively, secondary MPs originate from large plastic material. Human activities
205 or natural weathering processes have resulted in plastics breaking down to micro- or nano-
206 sized particles (Chamas et al., 2020). Tire wear and tear is a stealthy source of MPs in the
207 environment (Capolupo et al., 2020). Photo-oxidative and thermo-oxidative degradation,
208 mechanical degradation, hydrolysis, and microbial activity are all examples of natural
209 processes that enhance the formation of secondary MPs (Auta et al., 2017). Ultraviolet
210 (UV) light causes photo-oxidative degradation (which can lead to thermo-oxidative
211 degradation), and is a significant factor in the formation of MPs (Andrady, 2011).
212 However, these processes are location dependent, as MPs on land have greater degradation
213 than those in the water (Anderson et al., 2016). Differences in photo-oxidative degradation
214 are primarily due to the reduced temperature and oxygen content caused by the surrounding
215 water. Furthermore, water conditions promote biofilm accumulation onto the surface of the
216 plastic (Andrady, 2011; Bähler et al., 2020). Although biofilm may reduce UV degradation
217 by forming a barrier to sunlight, certain microorganisms can contribute to the

218 biodegradation of plastics (Oberbeckmann et al., 2015). Some MPs can breakdown by
219 hydrolysis, but it is not considered a significant mechanism in oceans (Andrady, 2011).
220 Marine conditions will form secondary MPs through wave action (e.g., surf or swash zone),
221 or sediment and wind abrasion (Efimova et al., 2018). Storm conditions further amplify the
222 degradation of plastics in the marine environment.

223 **2.3 Inputs of microplastics in aquatic environments**

224 Pathways in which MPs enter the aquatic environment include direct input, or from
225 terrestrial or atmospheric routes (Auta et al., 2017). **Table 1** provides examples of the
226 average concentrations of MPs sampled from aquatic environments, and their suggested
227 sources. Many products contain plastic, and these can directly end up in waterways, lakes,
228 and oceans through careless handling and littering, especially from recreational water
229 products (e.g., boats, fishing gear, or plastic toys used at the beach) (Sun et al., 2019). They
230 can also indirectly enter aquatic environments through littering, illegal dumping, and poor
231 management of landfills (Cole et al., 2011). Paint chips from boats or ships, and fibers from
232 marine ropes or nets for aquaculture also contribute to water MP pollution (Duis and Coors,
233 2016). Besides serving as a sink for MPs, WWTPs can also be a potential point source of
234 MP exposure for aquatic environments through effluent discharge (Kazour et al., 2019). A
235 study by Edo et al. (2020) predicted that 300 million MP debris were released into a nearby
236 river per day through effluent discharge. Furthermore, MPs can be transported from
237 terrestrial to aquatic environments through run-off, erosion, and wind (Rezaei et al., 2019).
238 Terrestrial inputs of MPs usually contained land applications of biosolids and soil mulching
239 (Campanale et al., 2020). Storm events can increase the concentration of land-based MPs
240 that reach aquatic environments (Eerkes-Medrano et al., 2015). Another input that is

241 receiving more attention in recent years is the atmospheric deposition of MPs (Murphy et
242 al., 2016). Although higher concentrations of airborne MPs are reported in urban
243 environments, the proximity of coastal cities to water sources could lead to increased levels
244 of MPs in rivers and oceans (Dris et al., 2016). Furthermore, long-range atmospheric
245 transport has been reported as an important factor for the concentration of MPs in the Arctic
246 region (Bergmann et al., 2019). Overall, the extent of MP contamination is evident by the
247 abundance of these particles, even in remote locations such as the Arctic (Bergmann et al.,
248 2019; Peeken et al., 2018).

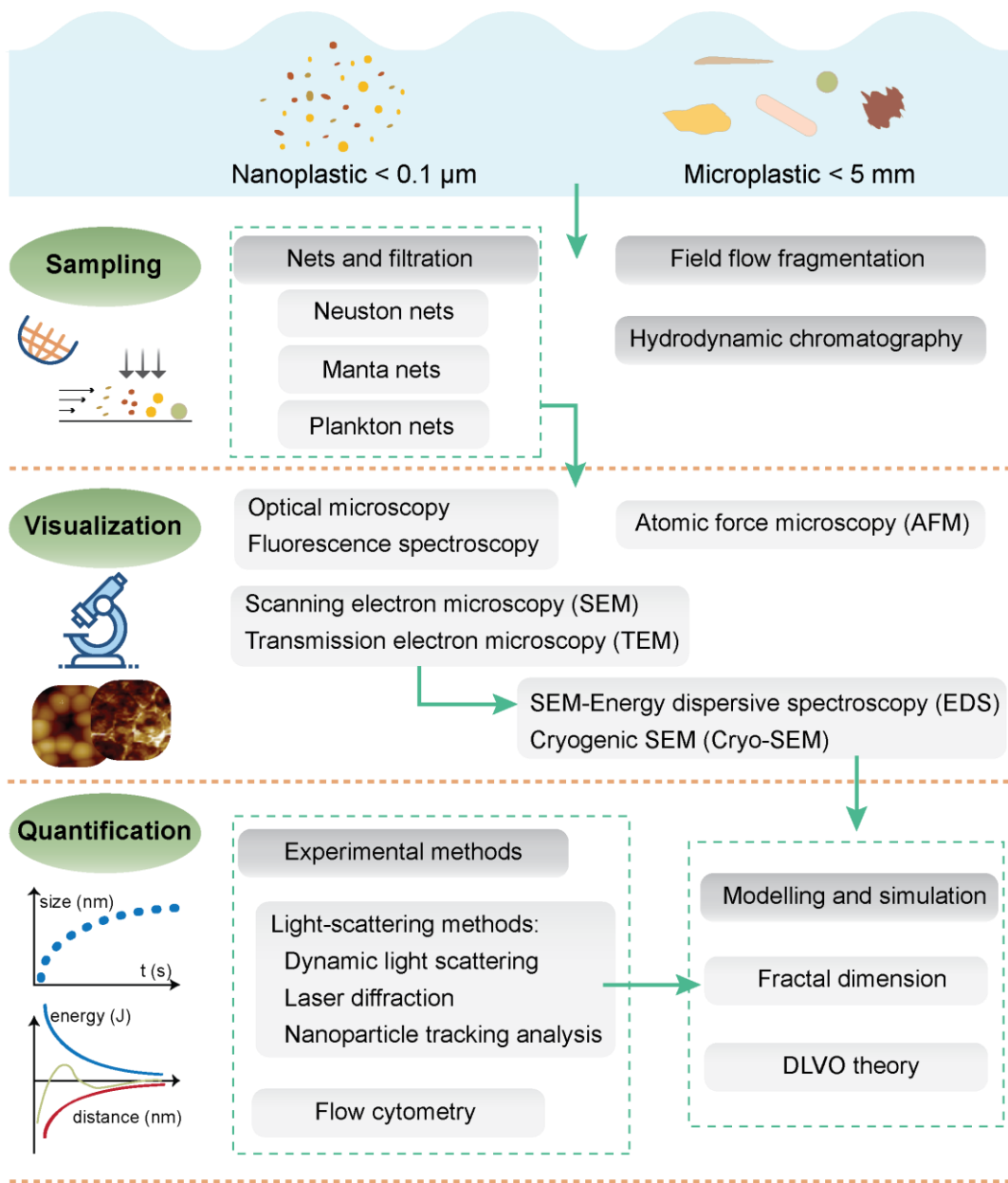
249 **Table 1** Sources and concentrations of microplastics in aquatic environments.

Continent	Location	Suggested Sources	Average MP Concentration	Sample Year	Reference
Antarctica	Ross Sea	WWTPs, ship traffic, research activities, ocean currents, and unknown	0.17 MPs·m ⁻³	2010	(Cincinelli et al., 2017)
Asia	29 rivers in Japan	Urban living, WWTPs, airborne (e.g., winds), and rainfall run-off	0 to 4.94 MPs·m ⁻³	2015-2018	(Kataoka et al., 2019)
	Nakdong River	Atmospheric fallout, heavy rain, run-off, urban living, and WWTPs	1555 MPs·m ⁻³	2017	(Eo et al., 2019)
Australia	GMA / Goulburn River Catchment	Natural processes	0.40 MPs·L ⁻¹	2018	(Nan et al., 2020)
Europe	Henares River	WWTPs	350 MPs·m ⁻³	2019	(Edo et al., 2020)
	Le Havre harbor	WWTPs	~0.1-1.8 MPs·L ⁻¹	2018	(Kazour et al., 2019)
	Lake Bolsena	Airborne (e.g., winds), storms, land-based sources, and WWTPs	3.02 MPs·m ⁻³	2014	(Fischer et al., 2016)
	Lake Chiusi	Water circulation, WWTPs, and local fisheries	2.22 MPs·m ⁻³	2014	(Fischer et al., 2016)
	Ofanto River	Land-based sources (e.g., agricultural activities, run-off, and erosion)	~6 MPs·m ⁻³	2017-2018	(Campanale et al., 2020)
	Rhine River	Urban living, WWTPs, and ship traffic	892,777 MPs·km ⁻²	2014	(Mani et al., 2015)
	River Clyde	WWTPs	0.25 MPs·L ⁻¹	Not mentioned	(Murphy et al., 2016)
North America	Lake Winnipeg	Synthetic textiles, secondary MPs, atmospheric fallout, urban living, and WWTPs	193,420 MPs·km ⁻²	2014-2016	(Anderson et al., 2017)
	Raritan River	WWTPs	~30 MPs·m ⁻³	2015	(Estahbanati and Fahrenfeld, 2016)
	Chicago River	WWTPs	17.9 MPs·m ⁻³	2013	(McCormick et al., 2014)

250 *Note: Microplastics (MPs), Greater Melbourne Area (GMA), Wastewater Treatment Plants (WWTPs)*

251 **3. Analytical methods for studying microplastic aggregation in aquatic environment**

252 The physiochemical properties of MPs including color, shape, density (0.9-2.3 g·cm⁻³), and chemical constituents vary significantly in the environment, which increase the
253 difficulty to detect and quantitatively estimate the aggregation state of MPs in real water
254 environment (Stock et al., 2019). Generally, the analytical procedures for MP aggregation
255 in water environments include collection of samples to cover the full-size range of MPs,
256 their visualization, and quantification, as shown in **Fig. 2**. A convincing analysis of MP
257 aggregation requires standardized methods, which can be useful for understanding the
258 aggregation of MPs in water environments and maximize comparability of investigations.
259 A number of systematic methodologies for this purpose has been compared and
260 summarized in this section.
261



262

263 **Fig. 2.** Analysis processes for the aggregation of microplastics (MPs) in water including
 264 the sampling, visualization and quantification of MP' particle sizes.

265 **3.1 Microplastic sampling methods**

266 Sampling MPs in water environment is the first step for investigating the aggregation
 267 of MPs (Pico and Barcelo, 2019). To the best of our knowledge, most studies regarding
 268 water sample collection focused on quantifying the content of MPs in natural waters
 269 (Cutroneo et al., 2020). Some sampling and separation methods were also suitable for

270 investigating the aggregation state of MPs in natural waters.

271 The sampling methods of MPs in water can be divided into the selective, bulk sampling,
272 and volume-reduced methods (Wang and Wang, 2018; Zobkov and Esiukova, 2018).
273 Selective sampling refers to direct collection of plastic particles, and they are recognizable
274 by naked eyes (particles between 1 and 5 mm) (Silva et al., 2018; Zobkov and Esiukova,
275 2018). This technique is simple but misses some MPs when they are mixed with other
276 debris, or when they have no characteristic shapes, or with ultra-small size (Wang and
277 Wang, 2018). Bulk sampling refers to collecting the entire volume of water samples
278 containing the whole size range of MPs (Silva et al., 2018). Bulk sampling captures
279 relatively small amount of a sample that probably have low concentration of MPs for
280 subsequent processing and detection (Zobkov and Esiukova, 2018). Volume-reduced
281 sampling refers to the condensation of volume of sample, preserving only the portion of
282 interest for further processing (Silva et al., 2018). Therefore, the condensation of MPs
283 improves their mass concentration for stability assessment by instruments (Zobkov and
284 Esiukova, 2018). Selective and bulk sampling methods are usually used to collect sediment
285 samples or water samples, and the volume-reduced method seems to be the most frequently
286 applied approach for sampling water samples (Wang and Wang, 2018).

287 **Table 2** Advantages and disadvantages of various sampling methods for microplastics (MPs) from water

Method	Size range	Advantages	Disadvantage	Ref.
Neuston nets and Manta trawls	64-5000 μm	<ul style="list-style-type: none"> • Sample large volumes of water quickly • Easy to operate • Surface water is collected for floating MPs • Collect large number of MPs 	<ul style="list-style-type: none"> • Clogging of nets by organic or mineral materials • Potential contamination by tow ropes or containers 	(Cutroneo et al., 2020; Hidalgo-Ruz et al., 2012; Pico et al., 2019)
Plankton nets	50-500 μm	<ul style="list-style-type: none"> • Sample medium volumes of water • Easy to operate • Water column is collected • Quick to use 	<ul style="list-style-type: none"> • Clogging of nets by organic or mineral materials • Expensive and time-consuming 	(Cutroneo et al., 2020; Estahbanati and Fahrenfeld, 2016; Pico et al., 2019)
Filtration	100, 20 and 5 μm	<ul style="list-style-type: none"> • Easy to operate • Known water volume • Choice of filter pore sizes 	<ul style="list-style-type: none"> • Obstruction by organic or mineral matter • Sample low volumes of water • Potential contamination by the apparatus • Time consuming and laborious depending on pore sizes 	(Stock et al., 2019)
Field flow fractionation	1 nm-100 μm	<ul style="list-style-type: none"> • No stationary phase improved separation resolution • Coupled detectors • Cover the whole nanometer range 	<ul style="list-style-type: none"> • Hard to operate • Expensive (advanced instruments) • Low recovery and analysis speed • Hard to analyze environmental samples (need pretreatment) • Membrane limitation 	(Shendruk and Slater, 2012; Shendruk et al., 2013)
Hydrodynamic chromatography	5 nm-1.2 μm	<ul style="list-style-type: none"> • Rapid separation of particles • Higher recovery than field flow fractionation • Coupled detectors • Less interaction with stationary phase 	<ul style="list-style-type: none"> • Hard to operate • Expensive (advanced instruments) • Low separation resolution 	(Blom et al., 2003; Schwaferts et al., 2019)

288

289 **3.1.1 Nets and filtration**

290 Nets are the most frequently used devices for sampling MPs from waters (Hidalgo-
291 Ruz et al., 2012; Pico et al., 2019). This method is advantageous for covering large
292 sampling areas, filtering large volumes of water rapidly and concentrating MPs directly
293 during sampling (Stock et al., 2019). However, this method is difficult to apply in narrow
294 spaces such as pot basins, little channel, or in the presence of obstacles (Cutroneo et al.,
295 2020). Besides, the mesh size results in the omission of lower size fractions of MPs
296 (Zobkov and Esiukova, 2018). Nets with a mesh width of 50-3000 μm were often used,
297 and $\sim 300 \mu\text{m}$ was the most commonly employed size (Stock et al., 2019). Various types of
298 nets were used across studies (Cutroneo et al., 2020). For example, manta nets and neuston
299 nets with mesh sizes ranging from 64-5000 μm are used for surface water sampling
300 (Cutroneo et al., 2020; Hidalgo-Ruz et al., 2012; Pico et al., 2019). Plankton nets with
301 smaller mesh sizes (c.a. 50-500 μm) are used for water columns, and can have 30 times
302 higher recovering concentration than manta nets (Prata et al., 2019). For riverbed or seabed
303 sampling, drift or benthic nets that can be attached to the ground were used, while bongo
304 nets were used for sampling from mid-water levels (Stock et al., 2019). Manta nets, neuston
305 nets and plankton nets are the most frequently used devices, and a summary of their
306 comparative performances is given in **Table 2**.

307 For the filtration method, MPs are separated by passing the water samples over a filter,
308 usually aided by a vacuum. To sort out larger particles before the filtration step, water
309 samples can first be passed through a sieve with 500 μm mesh size. The size of MPs
310 retained and the filterable volume are a direct consequence of the filter pore size used (Sun
311 et al., 2019). A promising method is filtering of large volumes of water samples via

312 cascades of 100, 20 and 5 μm filters by directly fractionated pressure filtering (Stock et al.,
313 2019). This method facilitates the simultaneous collection of different size fractions of MPs
314 down to $< 5 \mu\text{m}$, and enables a comprehensive resolution of the size spectrum of MPs
315 (Stock et al., 2019; Sun et al., 2019).

316 Nets and filtration methods can maintain the original aggregation state of MPs (Lenz
317 and Labrenz, 2018). However, when these two methods are used, we must balance between
318 the filters' ability to obtain MPs and potential clogging of pores by organic matter, mineral
319 matter and microorganisms (Pico et al., 2019; Stock et al., 2019). The sequential filtration
320 using filters with smaller pore sizes might minimize the clogging (Pico and Barcelo, 2019).
321 In addition, the above two methods would lose the nanometer-sized particles because of
322 their sorption on filters or pore limitations (Sun et al., 2019).

323 **3.1.2 Field flow fractionation (FFF)**

324 Beyond the above fractions with large particle sizes, there are smaller plastic
325 fragments that are $< 1 \mu\text{m}$ (Pico and Barcelo, 2019). Chromatographic techniques including
326 passive and active separation are typically applied to collect the micro- or nano-sized
327 plastics (Fu et al., 2020). Field flow fractionation (FFF) is a representative active separation
328 technique that can be used for separating MPs with size of 1 nm - 100 μm from water
329 samples (Shendruk and Slater, 2012; Shendruk et al., 2013). Particles such as colloids and
330 macromolecules are size-separated in a channel with parabolic and laminar flow under a
331 perpendicular external field (Shendruk and Slater, 2012). The nature of external fields (i.e.,
332 thermal, sedimentation, flow, gravitational, electrical, and magnetic) defines the type of
333 FFF (Messaud et al., 2009). Thermal FFF is suitable for separating polymers based on both
334 molecular weight and composition differences (Runyon and Williams, 2011).

335 Sedimentation FFF is an alternative to density separation of MPs by electrolytes
336 (Huppertsberg and Knepper, 2018). Flow FFF is most commonly applied method in the
337 separation and analysis of MPs with two modes: normal mode where larger particles have
338 longer retention, whereas this is reversed for larger particles in the steric mode (Gigault et
339 al., 2017; Huppertsberg and Knepper, 2018; Mintenig et al., 2018). Flow FFF technique
340 does not require a stationary phase, which reduces variations or errors caused by the
341 interaction with stationary phase (Shendruk and Slater, 2012). However, low recovery of
342 MPs exists for the flow FFF technique and an advanced instrument is indispensable
343 (Mintenig et al., 2018).

344 Asymmetrical flow field-flow fractionation (AF4) that belongs to flow FFF is
345 primarily used to characterize polymers (Fraunhofer et al., 2004). AF4 was applied to
346 characterize the size distribution of PS NPs and separate them in fish (Correia and
347 Loeschner, 2018; Gigault et al., 2017). AF4 was superior when tissues had auto-
348 fluorescence property that might interfere with the results of fluorescence microscopy and
349 flow cytometry (FCM) (Correia and Loeschner, 2018). However, AF4 cannot detect
350 polyethylene (PE) NPs in fish due to the interference of light-scattering background,
351 indicating that AF4 requires further adjustment for analyzing different types of NPs
352 (Correia and Loeschner, 2018). AF4 coupled to pyrolysis gas chromatography-mass
353 spectrometry can determine particle sizes and polymer types of MPs, which contributed to
354 a framework development for standardizing the measurement method of MP sizes
355 (Mintenig et al., 2018). Furthermore, hollow fiber flow field-flow fractionation coupled
356 with UV-Vis detector can characterize the particle size distribution of poly(vinyl acetate)
357 NPs in aqueous suspensions (Xiao et al., 2018).

358 **3.1.3 Hydrodynamic chromatography (HDC)**

359 Hydrodynamic chromatography (HDC) is a passive separation technique that can be
360 applied for MP separation from water samples for particle sizes in the range from 10 nm to
361 1 μm (Lespes and Gigault, 2011). The HDC separation principle relies on the size-
362 dependent exclusion from the wall in a channel where a pressure-driven flow is applied
363 (Lespes and Gigault, 2011). Separating components of sample mixtures is accomplished
364 by parabolic flow velocity gradients that develop within the column between a packed bed
365 filled with media grains (Shendruk and Slater, 2014). The movement of particles with size
366 range from 10 nm to 1 μm under the Brownian motion can be disturbed by media grains
367 (Fu et al., 2020). Small particles receive increasing hydrodynamic effect and van der Waals
368 interactions with media grains and migrate closer to the channel wall, which is subjected
369 to a lower flow velocity (Cejas et al., 2018). Larger particles stay close to the center of the
370 channel where the higher flow velocity causes them to move faster (Liu et al., 2013). Thus
371 small particles elute slower than large particles (Shendruk and Slater, 2014).

372 HDC has been employed to separate MPs and NPs from sediment, seawater and food
373 (Bouwmeester et al., 2015; Chain, 2016). HDC coupled with other detectors has also been
374 used for separation (Philippe et al., 2014; Pirok et al., 2017). For example, HDC coupled
375 with UV-vis detector or ICP-MS was employed to separate PS NPs and several metal
376 nanoparticles in aqueous suspensions (Philippe et al., 2014). HDC combined with size-
377 exclusion chromatography was used to obtain information on the two-dimensional particle
378 size distribution of the mixed suspensions between PS NPs and polyacrylate NPs (Pirok et
379 al., 2017). HDC showed rapid separation and better recoveries than AF4, but the separation
380 resolution was lower than that of FFF (Revillon, 2000).

381 **3.2 Microplastic visualization methods**

382 After sampling MPs, various visual sorting methods are applied to provide the
383 stability information of MPs as single particles, homoaggregates or heteroaggregates with
384 other materials, such as suspended sediments, algae, and bacteria (Bäbler et al., 2020;
385 Sendra et al., 2019; Sun et al., 2018). This is frequently conducted by direct observation by
386 naked eyes or assisted by a microscope (Silva et al., 2018). For example, the
387 homoaggregation of PE MPs with diameters of 1-5 mm was observed by naked eyes and
388 recorded with a digital camera (Li et al., 2019). To obtain more detailed information on MP
389 aggregation in a water sample, optical microscopy, electron microscopy and scanning
390 probe microscopy are utilized. These microscopes based on different operation modes offer
391 direct access to the geometry and surface characteristics of MP samples (Schwaferts et al.,
392 2019).

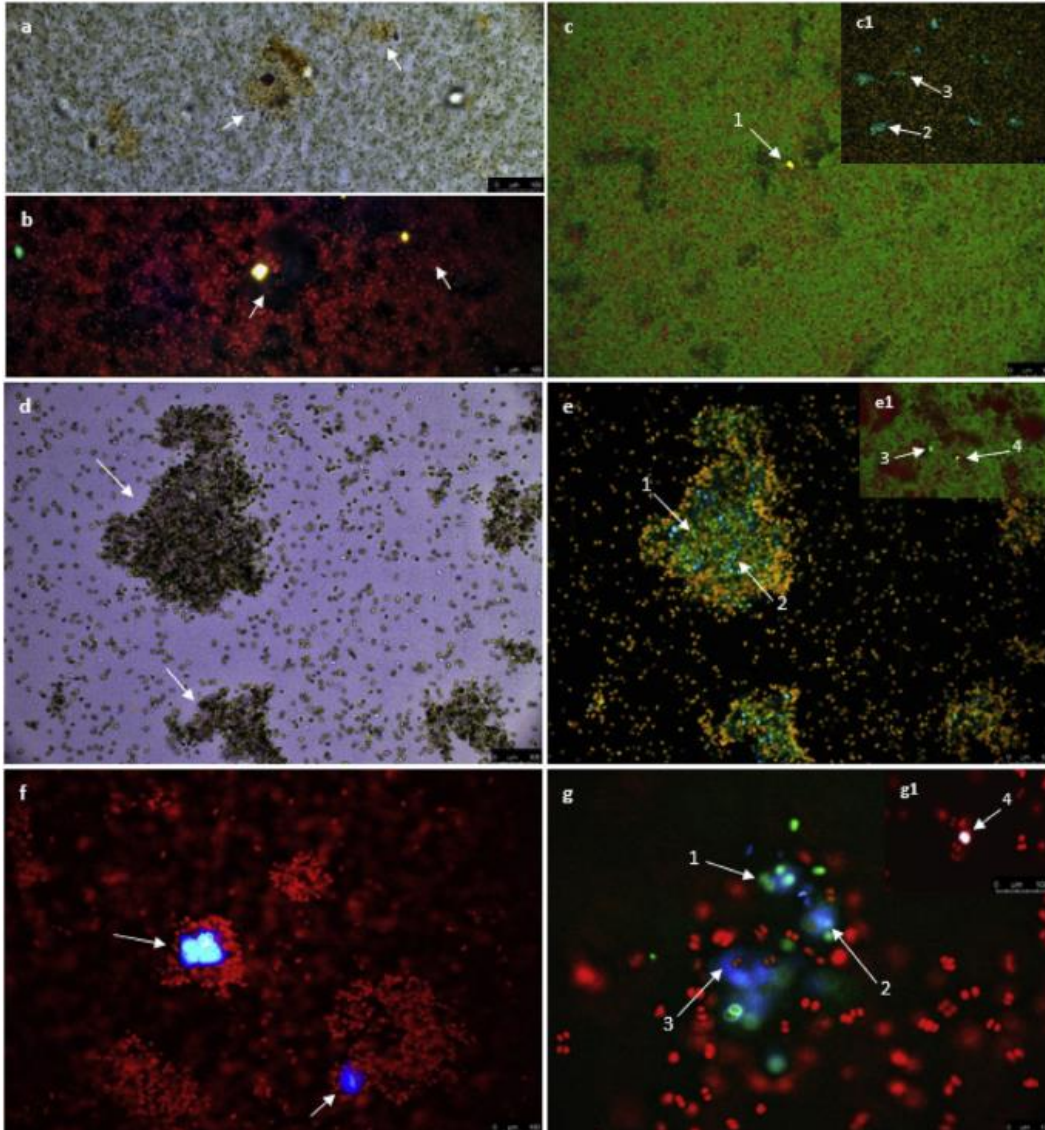
393 **3.2.1 Optical microscopy**

394 Optical microscopes are usually applied for providing the surface texture, structural
395 information and number of particles with micrometer size (Silva et al., 2018). The
396 heteroaggregates between suspended sediments and PE MPs with diameters ~2 mm were
397 directly observed by optical microscopes (Li et al., 2019). Techniques such as fluorescence
398 spectroscopy can analyze fluorescently marked particles or materials emitting sufficient
399 fluorescence signal, which could facilitate the investigation of the homoaggregation of MPs
400 or their heteroaggregation with other particles in natural waters (Cunha et al., 2019).

401 For example, fluorescence spectroscopy was applied to compare the homoaggregation
402 of fluorescent PS NPs and their heteroaggregation with suspended sediment in different
403 water chemical conditions (Li et al., 2019). In 500 mM NaCl solution, fluorescent PS NPs

404 with diameter of 100 nm were found to attach onto the surface of suspended sediment with
405 sizes greater than plastic particles (100~500 μm) in the presence or absence of humic acid
406 (HA). By contrast, no homoaggregation or heteroaggregation of PSNPs with suspended
407 sediment was observed in $10 \text{ mg}\cdot\text{L}^{-1}$ HA solutions. This was primarily because HA could
408 be adsorbed onto PS NP and sediment surfaces, imparting electrostatic repulsion and
409 hinderance forces, and thus increased the stability of PS NPs (Tallec et al., 2019). PS and
410 poly(methyl methacrylate) (PMMA) MPs were stained with Nile Red, and applied to
411 characterize their heteroaggregation with microalgae through fluorescence microscopy
412 (Cunha et al., 2019). As shown in **Fig. 3**, two freshwater microalgae (*Scenedesmus sp.* and
413 *Microcystis panniformis*) and two marine microalgae (*Gloeocapsa sp.* and *Tetraselmis sp.*)
414 excreted exopolymeric substances (EPS) and colonized MPs. The heteroaggregation
415 degree was related to MP' type, size and density as well as the yield of EPS that was
416 species-specific.

417 However, fluorescence spectroscopy is not applicable for environmental MPs because
418 the dye or fluorophores are not plastic-specific (Schwaferts et al., 2019). Further studies
419 are suggested to focus on the interaction between dyes and MPs, which may facilitate the
420 application of plastic-specific and plastic-sensitive dyes and dye combinations. Another
421 drawback of visual sorting is the size limitation, i.e., particles below a micrometer is
422 difficult to visually discriminate from other materials. Smaller MPs and NPs should
423 generally be sorted out using electron microscopy or scanning probe microscopy (Hale,
424 2017).



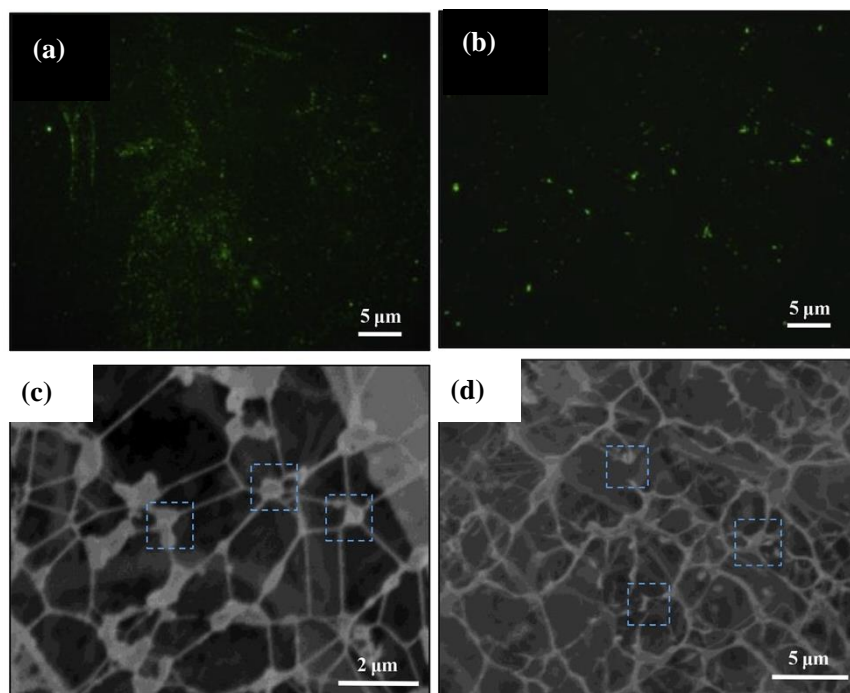
425
 426 **Fig. 3.** (a) Bright field micrograph of *Microcystis panniformis* heteroaggregates; (b) Same
 427 micrograph seen in (a), but under DAPI filters, being visible in the incorporation of the
 428 fluorescent microplastics (MPs) in the heteroaggregates; (c) Micrograph of *Scenedesmus*
 429 *sp.*, under I3 filters, showing the abundance of exopolymeric substances (EPS) and the MPs
 430 aggregation; (c1) Micrograph of *Scenedesmus sp.* under DAPI filters, exhibiting
 431 aggregation of different MPs. Each arrow pointing at yellow (1) and blue (2) represents
 432 polystyrene (PS). Each arrow pointing at the green (3) and purple (4) represents
 433 poly(methyl methacrylate) (PMMA); (d) Bright field micrograph of *Tetraselmis sp.*
 434 Heteroaggregates; (e) Same micrograph seen in (d), but under DAPI filters, showing
 435 heteroaggregates composed of microalgae (orange) and MPs (blue/green) and EPS; (e1)
 436 Micrograph of *Tetraselmis sp.* heteroaggregates, under I3 filters; (f) Micrograph of
 437 *Tetraselmis sp.* showing the colonization of MPs by the microalga, under DAPI filters;
 438 (g/g1) Micrographs of MPs aggregate with *Gloeocapsa sp.*, under DAPI filters. Graph was
 439 cited and reproduced from ref. (Cunha et al., 2019) with permission.

440 3.2.2 Electron microscopy

441 By means of electron beams, the resolution of electron microscopy is much higher
442 than optical microscopy, spanning the range from 1 nm to millimeters (Schwaferts et al.,
443 2019). Scanning electron microscopy (SEM) and transmission electron microscopy (TEM)
444 are often applied to provide high-resolution images, characterize the precise size, and
445 facilitate the differentiation of MP homoaggregates and heteroaggregates with Fe₂O₃,
446 alginate, soil particles, and other solid particles (Liu et al., 2019a; Oriekhova and Stoll,
447 2018).

448 The interaction between MPs and microalgae was mostly analyzed by SEM and TEM,
449 as shown in **Fig. 1**. For example, microalgae (*Chlamydomas reinhardtii*) colonized MPs
450 (polypropylene (PP) and high-density polyethylene), and the heteroaggregates constituted
451 by microalgae, MPs and EPS were observed by SEM (Lagarde et al., 2016). The formation
452 of heteroaggregation between TiO₂ nanoparticles and PS MPs in water was confirmed by
453 SEM, which decreased the toxicity of TiO₂ nanoparticles to marine algae *Chlorella sp.*
454 (Thiagarajan et al., 2019). TEM was applied to characterize the particle size distribution
455 and mean sizes of polyvinyl chloride (PVC) MPs (Zhang et al., 2017). TEM images showed
456 that PS beads attached on the surface of marine bacterium *Halomonas alkaliphila* led to
457 cellular membrane damage and death (Sun et al., 2018). Although most MPs with a wide
458 size range could be observed by TEM or SEM, these two methods require dry sample
459 preparation, which may induce deposition and interfere with the aggregation state of MPs
460 (Schwaferts et al., 2019). These two methods also need a long analysis time and limited
461 sample sizes or numbers to be studied, which make the results random and thus unreliable
462 (Fu et al., 2020).

463 TEM and SEM can be coupled with other instruments to provide details about the MP
464 aggregation state. Energy dispersive spectroscopy (EDS) provides the elemental
465 information of samples via detecting the characteristic X-rays emitted from the elements
466 within the sample by the electron beam (Schwaferts et al., 2019). The SEM-EDS was able
467 to distinguish the homoaggregation of MPs, and heteroaggregation between MPs and DOM
468 or inorganic minerals in real water samples (Fu et al., 2020). Cryogenic SEM (Cryo-SEM)
469 was used to directly observe the aggregation state of PS NPs in the mixture of DOM and
470 salt solution (Cai et al., 2018). As shown in **Fig. 4**, Cryo-SEM images clearly show the
471 formation of PS NPs-DOM clusters through the bridging effect in the mixture of DOM and
472 FeCl₃. Cryo-SEM method maintained the morphology of samples in their native
473 environment by rapid freezing, which is a promising tool to reveal the precise information
474 of aggregation state (Kaberova et al., 2020). However, Cryo-SEM may face challenges
475 including low image contrast and low signal to noise ratio.



476

477 **Fig. 4.** Fluorescence images (a, b) and Cryo-SEM images (c, d) of polystyrene nanoplastics
 478 in 1 mM FeCl₃ and Suwannee River humic acid (a, c) or Suwannee River fuvic acid (b, d)
 479 solutions. Graph was cited and reproduced from ref. (Cai et al., 2018) with permission.

480 3.2.3 Scanning probe microscopy

481 Scanning probe microscopy, especially atomic force microscopy (AFM), has been
 482 identified as one of the most powerful techniques for providing images at nanoscale
 483 resolutions (Stawikowska and Livingston, 2013). AFM has been proven useful in the
 484 assessment of in-situ surface properties of particles at both microscale and nanoscale (Fu
 485 et al., 2020). More importantly, the original dispersed states can be preserved during the
 486 AFM analysis process as samples can be placed in vacuum, gaseous, or aqueous
 487 environments with desirable conditions, thereby reducing potential experimental artifacts
 488 on samples during the preparation process (Fu et al., 2020). AFM provides an effective and
 489 non-destructive means for nanoparticle characterization and surface properties analysis
 490 such as force profiles, which could also be applied for investigating the stability of MPs
 491 (Fu and Zhang, 2018). For example, AFM images indicated that the surface morphology

492 of particulate plastics was altered by the formation of PP-bacteria heteroaggregates
493 (Kumari et al., 2018). Ruiz-Cabello et al. (2013) employed AFM to measure direct force
494 profiles between carboxyl-modified latex particles (diameter 1.0 μm) in different
495 electrolyte solutions (KCl, MgCl₂, LaCl₃, ZrCl₄) and used the observed force profiles to
496 predict their aggregation rates. The force profiles fitted well with Derjaguin-Landau-
497 Verwey-Overbeek (DLVO) theory even though some non-DLVO forces also existed
498 (Trefalt et al., 2017).

499 Visualization methods are commonly applied by most researchers to identify MP
500 aggregation in natural waters. However, visual examination may provide inaccurate
501 information on MP aggregation because it is difficult to differentiate plastic particles from
502 other organic or inorganic particles with similar sizes or shapes (Hale, 2017). Additional
503 techniques such as Raman spectroscopy, Fourier-transform infrared spectroscopy (FTIR),
504 liquid chromatography, and pyrolysis gas chromatography coupled to mass spectrometry
505 are required to be applied to identify the chemical composition of MPs, in addition to the
506 use of visualization methods (Schwaferts et al., 2019).

507 **3.3 Microplastic aggregation quantification methods**

508 **3.3.1 Experimental methods**

509 3.3.1.1 Light-scattering methods

510 Light-scattering methods are widely used to quantify the in-situ aggregation behavior
511 of MPs since it is non-destructive (Yu et al., 2019). The most frequently applied light-
512 scattering method, dynamic light scattering (DLS) instrument, determines the time-
513 dependent hydrodynamic diameter (D_h) of sample with size range from 0.6 nm to 6 μm
514 under the Brownian motion (Kastner and Perrie, 2016). The zeta potential and

515 electrophoretic mobility of MPs in an applied electric field can be measured by detecting
516 frequency shifts in the scattered light, which is important for predicting MP aggregation
517 behavior (Kaszuba et al., 2010). So far, there have been a large amount of studies using
518 DLS to measure the aggregation kinetics, aggregate size, and zeta potentials of MPs/NPs
519 in various water chemical conditions (Cai et al., 2018; Yu et al., 2019). Although DLS is
520 fast and simple operation, it has disadvantages such as low resolution and low accuracy for
521 large particles (Wang et al., 2015). DLS is more appropriate for measuring monodisperse
522 suspensions, and has limitation in heteroaggregation studies (Praetorius et al., 2020).

523 Laser diffraction (LD) analyzer based on the static light scattering is used for
524 measuring particles with sizes ranging from submicron (500 nm) to millimeter (10 mm),
525 i.e., particles can have sedimentation process and their movement cannot only be governed
526 by Brownian motion (Kastner and Perrie, 2016; Schwaferts et al., 2019). LD relies on time-
527 averaged intensity measurements and uses volume mean diameter to represent the size of
528 particles (Praetorius et al., 2014). The distribution percentiles D(10), D(50) and D(90) can
529 be reported to analyze variation in particle sizes, representing the 10th, 50th, and 90th
530 percentile of particle size, respectively (Praetorius et al., 2014). The effects of monovalent
531 (KNO₃, NaNO₃ and NaCl) and divalent (CaCl₂ and BaCl₂) electrolytes with and without
532 HA in water on the aggregation kinetics of PS MPs (diameter of 17.9 μm) were investigated
533 by LD (Li et al., 2018). The results showed that divalent electrolytes were more efficient
534 in destabilizing PS MPs as compared to monovalent electrolytes due to the higher charge
535 neutralization effect of divalent cations (Qu et al., 2010). LD has been proposed as a
536 method to study heteroaggregation kinetics of nanoparticles with larger μm-sized

537 suspended particulate matters, which enables it to measure heteroaggregation of MPs
538 (Praetorius et al., 2020).

539 DLS and LD measurements probe the polydispersity index, of which the value >0.2
540 indicates a very broad size distribution, or heterogeneous or multimodal particle size
541 distributions (Li et al., 2019). The aggregation kinetics at an early stage and initial
542 aggregation rate were calculated using the DLS and LD data in most studies (Summers et
543 al., 2018). The initial aggregation rate constant of MPs (k) is proportional to the inverse of
544 MPs concentration (N_0) and the initial increase rate of the D_h with time (t), which is
545 calculated by eq 1 (Li et al., 2018).

$$546 \quad k \propto \frac{1}{N_0} \left(\frac{dD_h(t)}{dt} \right)_{t \rightarrow 0} \quad (1)$$

547 The attachment efficiency (α) is defined as the reciprocal of the stability ratio (W) and is
548 calculated by eq 2 (Praetorius et al., 2020):

$$549 \quad \alpha = \frac{1}{W} = \frac{k}{k_{fast}} = \frac{\frac{1}{N_0} \left(\frac{dD_h(t)}{dt} \right)_{t \rightarrow 0}}{\frac{1}{(N_0)_{fast}} \left(\frac{dD_h(t)}{dt} \right)_{t \rightarrow 0, fast}} \quad (2)$$

550 where, the subscript “fast” represents a favorable aggregation condition. The numerator
551 and denominator represent the aggregation rate constants under the reaction-limited
552 aggregation regime ($\alpha < 1$) and diffusion-limited aggregation regime ($\alpha = 1$), respectively
553 (Qu et al., 2010). The critical coagulation concentration (CCC) values of MPs can be
554 obtained from α . For instance, the CCC values of PS NPs were around 300 mM to 450 mM
555 in monovalent electrolytes (e.g., NaCl and KCl) and around 30 mM in divalent electrolytes
556 (e.g., CaCl₂ and BaCl₂) (Liu et al., 2019b; Yu et al., 2019). While for micro-sized PS MPs,
557 CCC value was smaller compared to PS NPs, such as around 15 mM in NaCl, KNO₃,
558 NaNO₃, and around 3 mM in CaCl₂ and BaCl₂ (Li et al., 2018). Besides, the addition of

559 HA resulted in CCC values of 1.03-2.15 times higher than that without HA, and the CCC
560 values were positively correlated to the HA concentrations (Li et al., 2018). This can be
561 attributed to the fact that HA could readily cover the MP surface via adsorption or
562 hydrophobic interaction, which might enhance the stability of MPs due to steric
563 stabilization and/or electrostatic repulsion (Qu et al., 2010).

564 LD or DLS is becoming a preferred technique for particle size measurement compared
565 to SEM, due to their short analytical time, high precision, reproducibility, flexible
566 operation, and easy application (Shekunov et al., 2006). However, significant error in
567 estimating the hydrodynamic particle size for non-spherical particles, such as films and
568 fibers exists in LD or DLS (Shekunov et al., 2006). By contrast, due to direct visualization,
569 SEM is more reliable in analyzing the particle size of non-spherical particles. But
570 characterizing particle size by SEM may have statistical biases associated with particle
571 aggregation during the drying process of sample preparation (Klang et al., 2012).

572 **Table 3** Comparison of light-scattering methods for investigating microplastic aggregation
 573 in water

Method	DLS	LD	NTA
Size range	0.6 nm ~ 6 μm	500 nm ~ 10 mm	10 nm ~ 1000 nm
Concentration range	Maximum 40 % w/v	Not defined; need low concentration of sample	10 ⁷ ~ 10 ¹⁰ particle·mL ⁻¹
Principle	Scattered light and Brownian motion	Laser diffraction	Scattered light and Brownian motion
Key parameters	<ul style="list-style-type: none"> • Average hydrodynamic diameter • Intensity, volume and number-based particle size distribution • Polydispersity index 	<ul style="list-style-type: none"> • Volume mean diameter • D(10), D(50) and D(90) • Polydispersity index 	<ul style="list-style-type: none"> • Particle concentration • Hydrodynamic diameter
Advantages	<ul style="list-style-type: none"> • Fast and simple operation • Aggregation rate measurement • Zeta potential measurement • Stability ratio measurement 	<ul style="list-style-type: none"> • Wide size range • Suitable for sedimentation • Aggregation rate measurement • More accurate in heterogeneous system • Stability ratio measurement 	<ul style="list-style-type: none"> • Provide particle number concentration • Provide size of individual particles • Video of particle motion
Limitations	<ul style="list-style-type: none"> • Low accuracy and resolution for large particles • Less suitable for heteroaggregation studies • Affected by light absorption of the medium 	<ul style="list-style-type: none"> • Affected by light absorption of the medium 	<ul style="list-style-type: none"> • The motion trail reduces accuracy • Operation difficult • Not suitable for particles that are too polydisperse or too close in size

574 Nanoparticle tracking analysis (NTA) comes to the forefront when studying poly-
 575 dispersed samples where a range of sizes is present, because the NTA data clearly indicate
 576 different sizes of particles in suspension (Fu et al., 2020). The detailed comparison of the
 577 three light-scattering methods are summarized in **Table 3**. NTA can simultaneously analyze
 578 the particle concentrations and particle size distributions of a sample (Gross et al., 2016).
 579 The individual particles from 10 to 1000 nm can be detected to give particle size
 580 distribution data under NTA (Fu et al., 2020; Gross et al., 2016). The formation of NP
 581 particles during the degradation of a PS coffee cup lid was observed, and the time-resolved

582 evolution of particle size distribution of PS NPs was measured by using NTA (Lambert and
583 Wagner, 2016). Additionally, NTA was combined with dark field microscopy to measure
584 the particle size distribution of nanoparticles with the resolution of *ca.* 20 nm (Wagner et
585 al., 2014).

586 3.3.1.2 Flow cytometry (FCM)

587 FCM detect the light scattering and fluorescence by laser excitation of samples with
588 fluorescence characteristics (natural or staining) in suspension when they pass through a
589 light beam (Adan et al., 2017). FCM is highly sensitive to detect samples with diameter of
590 0.5 - 20 μm and can be applicable to analyze particles as large as 100 μm in diameter
591 (Green et al., 2003). FCM has been widely used in characterizing and distinguishing
592 different cell types in heterogeneous cells, analyzing the size and volume of cells, and
593 analyzing the expression of intracellular molecules (Adan et al., 2017). Some functions are
594 capable of quantifying and characterizing MP aggregation in seawater and study their
595 distribution in the water column (Arias-Andres et al., 2018; Long et al., 2017). For example,
596 the aggregation state of MPs (diameter of 500 nm) in seawater was depicted by FCM
597 (Summers et al., 2018). The 500 nm MPs dispersed and slightly aggregate with the portion
598 of 39.9%. After 24 h seawater treatment, obvious aggregation could be detected because
599 the proportion of aggregated increased to 93.9%. FCM was also used to observe the
600 heteroaggregation between MPs and organisms such as phytoplankton, bacteria and algae
601 (Arias-Andres et al., 2018; Long et al., 2017). For instance, Long et al. (2017) used FCM
602 to verify the heteroaggregation between fluorescent MPs and phytoplankton (e.g., diatom
603 *Chaetoceros neogracile* and algae *Rhodomonas salina*), and measure the concentration of
604 MPs in the aggregates. The FCM approach was also used to quantify the amount of PS

605 MPs adsorbed on algal surfaces (Bhattacharya et al., 2010).

606 **3.3.2 Modelling and simulation for studying MP aggregation**

607 3.3.2.1 Fractal dimension

608 Apart from the aggregation kinetics of MPs, an in-depth study of the morphology and
609 structure of MP aggregates is required to determine the toxicity and fate of the aggregates
610 in aquatic environments (Quik et al., 2014). The aggregation of colloids leads to fractal
611 structures that exhibit fractal dimensions (D_f) from zero to three (Li and Logan, 2001). D_f
612 is defined by a power-law relationship between fractal aggregate mass (m) and aggregate
613 radius (r) (Quik et al., 2014).

$$614 \quad m \propto r^{D_f} \quad (3)$$

615 D_f can be determined from LD measurement, or optical sampling and digital image analysis
616 (Meng et al., 2013). D_f describes the geometry of aggregates, aggregation rate, and various
617 physical properties such as density and settling velocity of MP aggregates (Li and Logan,
618 2001; Long et al., 2015). The lower the aggregation rate, the more time particles have to
619 form a denser and more compact structure, and lead to a higher fractal dimension (Meng
620 et al., 2013). Long et al. (2015) used D_f to understand the structure of aggregates between
621 PS MPs and phytoplankton or algal species. They found that the heteroaggregate structure
622 turned less fractal after exposure to PS MPs. The correlation between sinking rates and
623 fractal aggregates can be illustrated by a fractal scaling model. In addition, D_f has been
624 applied to explain the compactness of MP homoaggregates and chitosan or alginate-
625 associated MP heteroaggregates in salt solution (Ramirez et al., 2016).

626 3.3.2.2 Derjaguin-Landau-Verwey-Overbeek (DLVO) theory

627 DLVO theory has been widely employed to understand the relationships between

628 colloids and their aggregation behavior, and it can be used to explain the stability of MPs
629 in water (Zhang, 2014). The classical DLVO theory considers van der Waals forces and
630 electrostatic forces for yielding the total interaction energies between the material surface
631 in contact (Wang et al., 2015). A particle-particle geometry was employed for
632 homoaggregation between MPs in aqueous environments because most studies used
633 commercial MPs with spheres shape (Cai et al., 2018). When investigating the
634 heteroaggregation between layered clay minerals and NPs in electrolyte solutions, a
635 particle-plate geometry was used because NPs behaved as small particles that deposited on
636 the surface of a large flat plate (Li et al., 2019). For the interaction energies between micro
637 or milli-sized MPs in water, a plate-plate geometry fitted well and elucidated the
638 aggregation behavior, such as the homoaggregation of PE MPs (diameter of 1 mm). DLVO
639 theory could also be employed to quantify the aggregation kinetics of MPs and estimate
640 their Hamaker constants (Romero-Cano et al., 2001). For example, the Hamaker constants
641 of PS NPs at different aging status derived from DLVO theory were found to decrease from
642 3.5 to 1.5×10^{-18} mJ after 3-day of UV irradiation (Liu et al., 2019b).

643 However, after release into aquatic environments, MPs are likely to undergo aging
644 process and as well as heteroaggregation with DOM, bio-colloids, and inorganic colloids,
645 which modify the surface properties of MPs and introduce non-DLVO forces between
646 particles (Alimi et al., 2018). DLVO theory failed to predict the stability of MPs when non-
647 DLVO forces (e.g., hydration forces, osmotic pressure, depletion attraction, or steric forces)
648 existed between two approaching particles or in multivalent electrolytes with high
649 concentrations (Wang et al., 2015). In this way, extended DLVO (eDLVO) theory was
650 proposed to model the complex systems. For example, eDLVO theory well explained the

651 aggregation of UV-aged PS NPs due to aging-induced increase in hydrophilicity (Liu et al.,
652 2019a).

653 **4. Factors affecting aggregation of microplastics**

654 The physicochemical properties (e.g., hydrophobicity, surface areas, and surface
655 charge) of MPs may change to some extent under the influence of their own properties, and
656 surrounding pH, light irradiation, solid constituents, and other factors (Jódar-Reyes et al.,
657 2006a; Wang et al., 2020). Therefore, the environmental conditions, coexisting solid
658 constituents as well as their own properties could affect the aggregation behavior of MPs
659 in aquatic environments (Jódar-Reyes et al., 2006a; Wu et al., 2019b). Few recent studies
660 pointing out the factors affecting the aggregation of MPs are summarized in **Table 4**.

661 **Table 4** Review of recent studies regarding the aggregation of microplastics

Parameter	Main findings	Ref
Particle size	Smaller MPs are more prone to aggregation at the same conditions. Larger PSNPs-COOH (200 nm) have higher stability than smaller PSNPs-COOH (50 nm) in CaCl ₂ solution. Smaller PS MPs (0.1-0.6 μm) aggregated rapidly than larger PS MPs (0.8-1.5 μm) in seawater.	(Dong et al., 2018; Song et al., 2019)
Composition	MP composition affects their homoaggregation and heteroaggregation with microalgae. PS NPs are more stable in water than PE NPs. The CCC values of PS NPs were 10 mM for CaCl ₂ , 25 mM for MgCl ₂ , and 800 mM for NaCl, whereas those of PE NPs were lower (e.g., 0.1 mM for CaCl ₂ , 3 mM for MgCl ₂ , and 80 mM for NaCl). The heteroaggregation process between MPs and microalgae was influenced by MP type and EPS excreted by microalgae.	(Cunha et al., 2019; Shams et al., 2020)
Surface modification	Surface modification changed the steric hinderance, hydrophilicity and electrostatic force of plastic particles, and further influenced the aggregation kinetics. The stability decreased in the order of bare PS NPs < PSNPs-NH ₂ < PSNPs-COOH due to the hydrophilic surface modifications.	(Yu et al., 2019)
Electrolyte type	Regardless the type of plastic particle (PS, PE), the CCC of MPs increased in the order of trivalent cation (FeCl ₃), divalent cations (e.g., CaCl ₂ , BaCl ₂ , MgCl ₂), and monovalent cations (e.g., NaCl, KCl). This phenomenon was similar to other colloids and followed the Schulze-Hardy rule.	(Liu et al., 2019b; Shams et al., 2020)
pH	pH influenced the surface charge and electrostatic repulsion of particles via affecting the ionization of surface groups and adsorption of ions. The aggregation rate of PE NPs remain constant from pH 2 to 9. The aggregation of PS NPs with or without surface group modified as the function of pH was different among previous studies.	(Romero-Cano et al., 2001; Shams et al., 2020; Skaf et al., 2020)

	<p>The concentration, size, and surface physiochemical property of DOM determine its impact on the plastic particle stability and mobility. DOM is one of the most significant factors affecting plastic particle aggregation in waters and may overwhelm the effect of physicochemical properties of plastic particle.</p>	
DOM	<p>DOM (e.g., humic acid and fulvic acid) destabilized MPs through the bridging effect or surface charge reverse and stabilized MPs through increasing steric repulsion and electrostatic repulsion.</p> <p>In NaCl solution, DOM stabilized PS NPs and PS-COOH. In CaCl₂ solution, DOM (< 5 mg·C·L⁻¹) inhibited the aggregation of PS NPs and PS-COOH and accelerated their aggregation when DOM concentration was higher than 5 mg·C·L⁻¹. In 1 mM FeCl₃ solution, DOM promoted the aggregation of PS NPs.</p>	(Song et al., 2019; Wang et al., 2020; Yu et al., 2019)
Surfactant	<p>Plastic particles (e.g., PE fibers and PS particles) were stabilized by surfactants. Different types of surfactants had different stabilization mechanisms. Anionic/cationic surfactants can add sufficient charges to the particle surface and shield the particle from the effect of solution pH changes. Nonionic surfactants rarely shifted the surface charges of particle, but provided steric hindrance force to stabilize particles.</p>	(Jódar-Reyes et al., 2006b; Romero-Cano et al., 2000)
Light	<p>Light can affect the aggregation of plastic particles through aging process. UV irradiation improved the stability of PSNPs in NaCl solution and promoted PSNP aggregation in CaCl₂ solution.</p>	(Liu et al., 2019b)
Other factors	<p>Phytoplankton, microorganisms (e.g., bacteria and algae), and inorganic colloids (e.g., clay, suspended sediments and Fe₂O₃) easily adhere to the surfaces of plastic particles and form heteroaggregates. EPS and the size of suspended sediment play an important role in the heteroaggregation processes of MPs. The MP- algae aggregation depends on the species and the physiological state of the algae.</p>	(Long et al., 2015; Mao et al., 2018; Singh et al., 2019; Zhang et al., 2017)

662 *Note: microplastics (MPs), critical coagulation concentration (CCC), dissolved organic matter (DOM), exopolymeric substances (EPS), polystyrene (PS),*
663 *polyethylene (PE)*

664 **4.1 Physicochemical properties of microplastics**

665 **4.1.1 Size**

666 Surface charge behavior, electronic structure, surface energy, and surface reactivity are dependent
667 on particle size, which can change the interaction forces between two approaching surfaces (Zhang,
668 2014). For example, smaller particles are easy to aggregate under a given condition than larger
669 particles because of the higher surface energy of the smaller particles (He et al., 2008). In artificial
670 seawater (35 practical salinity units (PSU)), smaller PS MPs (0.1, 0.4, 0.6 μm) aggregated rapidly with
671 sand, while no heteroaggregation occurred between larger PS MPs (0.8 or 1.5 μm) and sand (Dong et
672 al., 2018). This was primarily because larger PS MPs had higher negative surface charges (~ -30 mV)
673 compared to the smaller MPs (~ -25 mV). DLVO interaction profiles demonstrated that the energy
674 barriers between larger PS MPs and sand (161 $k_{\text{B}}\text{T}$ and 296 $k_{\text{B}}\text{T}$) were 1.5-18.5 times higher than that
675 between smaller PS MPs and sand (16 $k_{\text{B}}\text{T}$ to 108 $k_{\text{B}}\text{T}$). In low salinity seawater (0 - 3.5 PSU), neither
676 larger nor smaller PS MPs had interaction with sand because all PS MPs were highly negatively
677 charged with zeta potentials of $-40\sim-50$ mV (Wang et al., 2020). The DLVO interaction profiles
678 showed high interaction energy barriers (≥ 218 $k_{\text{B}}\text{T}$) existed between all PS MPs and sand (Dong et
679 al., 2018). Larger carboxyl-modified PS NPs (PSNPs-COOH) (diameter 200 nm) with high electrical
680 forces showed higher stability than smaller PSNPs-COOH (diameter 50 nm) in a CaCl_2 solution,
681 because increasing particle sizes led to the lower Gibbs free energy and reduced adsorption rate of
682 Ca^{2+} (Song et al., 2019).

683 **4.1.2 Composition**

684 Homoaggregation of MPs could differ due to MP chemical composition probably because the
685 Hamaker constant determining van der Waals forces was composition-dependent (Zhang, 2014).
686 Previous studies showed that PS NPs were more stable than PE NPs in a variety of electrolyte solutions
687 (NaCl , CaCl_2 , and MgCl_2) (Shams et al., 2020). The effect of MP composition on their

688 heteroaggregation behaviors with microalgae was also investigated. Microalgae could excrete viscous
689 EPS which favored the aggregation with MPs (Long et al., 2015). Cunha et al. (2019) compared the
690 interactions of PMMA MPs and PS MPs with four microalgae, including *Microcystis panniformis*,
691 *Scenedesmus sp*, *Tetraselmis sp*, and *Gloeocapsa sp*. They found that the formation of MPs-microalgae
692 heteroaggregates depended not only on MP type but also on the content and viscosity of EPS. Since
693 *Microcystis panniformis* produced the lowest amount of EPS with low viscosity, they were able to
694 form heteroaggregates with PMMA MPs. *Gloeocapsa sp*. had the capability to aggregate with both
695 PMMA MPs and PS MPs due to the abundant production of viscous EPS. Compared to PE MPs,
696 microalga *Chlamydomas reinhardtii* were more inclined to form heteroaggregates with PP MPs after
697 20 days because the EPS produced by the alga had a stronger adhesion to PP MPs than PE MPs
698 (Lagarde et al., 2016).

699 **4.1.3 Surface coatings**

700 Functionalization and/or incidental surface coatings are frequently used to stabilize MPs via
701 increasing the electrostatic, steric, or hydrophilic repulsion forces among the particles (Saavedra et al.,
702 2019). For instance, linear poly(ethylene imine) and poly(diallyldimethyl ammonium chloride)
703 improved the stability of sulfate-modified PS MPs in NaCl solution (Shams et al., 2020). The
704 negatively charged PSNPs-COOH rapidly formed aggregates of 1764 ± 409 nm size because of the
705 charge neutralization effect of cations in seawater, whereas positively charged amino-modified PS NPs
706 (PSNPs-NH₂) formed aggregates of only 89 ± 2 nm size (Alimi et al., 2018). The aggregation rate of
707 amidine-modified PS MPs was much faster than sulfate-modified PS MPs in NaCl solution because
708 the former had a weaker electrostatic repulsion than the latter (Montes Ruiz-Cabello et al., 2015).
709 Furthermore, HA was found to have greater destabilizing effects on PSNPs-NH₂ with positive charges
710 than PS NPs and PSNPs-COOH with negative surface charges (Wu et al., 2019a). This was mainly
711 because the negatively charged HA was absorbed on the particle surface, and thus the neutralization

712 effects were greater for positively charged PSNPs-NH₂ (Qu et al., 2010).

713 **4.2 Environmental conditions**

714 **4.2.1 Electrolyte concentration and valence**

715 Electrolyte concentration strongly affects the aggregation behavior of MPs in water by
716 influencing the surface charge of particles (Alimi et al., 2018). For instance, PS NPs of 100 nm size
717 remained stable in 0.01 mM FeCl₃ solution, but the particle size of PS NPs increased rapidly up to 350
718 nm with the FeCl₃ concentrations increasing to 0.1 and 1 mM (Cai et al., 2018). The enhanced
719 aggregation was mainly due to the compression of the electric double layer and charge shielding on
720 the surface of the particulate plastics, which weakened the repulsive forces between particles (Wu et
721 al., 2019a; Xiao et al., 2018). When the electrolyte concentration exceeded the CCC value, the
722 repulsive interactions were insignificant or absent (Li et al., 2018). As a result, the aggregation rate of
723 MPs changed slightly due to the fact that the aggregation changed from the reaction-limited
724 aggregation regime to the diffusion-limited aggregation regime (Xiao et al., 2018).

725 The valence of ions is also a key factor that controls the aggregation behavior of MPs in water
726 (Wang et al., 2020). For example, the CCC value of PS NPs in NaCl solution (800 mM) was 80-fold
727 and 32-fold higher than those in CaCl₂ (10 mM) and MgCl₂ (25 mM) solutions, respectively (Shams
728 et al., 2020). The CCC value of PE NPs in NaCl solution (80 mM) was 27-fold higher than that in
729 MgCl₂ solution (3 mM). The ion-valence-dependent effect usually follows the Schulze-Hardy rule,
730 which suggests that the aggregation state mainly depends on the ionic valence of the opposite charge
731 to that of colloids (Wu et al., 2019a; Xiao et al., 2018). The aggregation rates of sulfonate-modified
732 PS NPs with the diameter of 115 nm increased in the order of K⁺ < Mg²⁺ < La³⁺ (Schneider et al., 2011).

733 **4.2.2 Effect of pH**

734 The pH of the solution can influence the ionization of surface functional groups and surface
735 charge of MPs, which then determines the magnitude of the electrostatic repulsion, and thus affects

736 the aggregation behavior (Li et al., 2018). The pH in the aquatic environment typically remains
737 between 5 and 9 (Chowdhury et al., 2013). Isoelectric point or zero point of charge is the pH at
738 which the surface of particles has a net neutral charge (Bolan et al., 1999; Hierrezuelo et al., 2010).
739 Most MPs have no isoelectric point, or have isoelectric point below 3, which are away from pH
740 values in natural waters (Li et al., 2018; Skaf et al., 2020; Wang et al., 2020). Thus MPs can be
741 stabilized by electrostatic repulsive forces in the aquatic environment (Hierrezuelo et al., 2010). For
742 example, sulfate-modified PS NPs (100 nm diameter) had no isoelectric point and the particle sizes
743 changed slightly from pH 2.3 to 11 due to strong electrostatic repulsion between particles in
744 ultrapure water (Wang et al., 2020). Similarly, Shams et al. (2020) found that the particle size of PE
745 NPs remained statistically constant from 284.92 ± 140.56 nm to 310.29 ± 165.58 nm from pH 5 to
746 9 in 10 mM NaCl solution due to strong electrostatic repulsive forces. The hydrodynamic diameters
747 of PS NPs were constant (c.a. 900 nm) in these conditions. While some studies found that the
748 stability of PS NPs (100 nm diameter) and PSNPs-COOH (303 nm diameter) increased with
749 increasing pH in NaCl solution, because more hydroxyl groups could be adsorbed on particle
750 surfaces making the zeta potential values more negative and the electrostatic repulsion higher
751 (Romero-Cano et al., 2001). The discrepancy among these studies may rely on the different
752 production processes, which resulted in the differences of physicochemical properties of the
753 particles such as size, surface chemistry and heterogeneity (Praetorius et al., 2020).

754 **4.2.3 Effect of DOM**

755 DOM is ubiquitous in natural waters and can adsorb onto MP surfaces by hydrophobic interaction,
756 ligand exchange, and electrostatic interaction (Tallec et al., 2019). DOM may change the stability of
757 MPs and make them aggregated or dispersed variably in natural waters depending on the valence of
758 ions and functional groups on MP surface (Cai et al., 2018). Adsorbed DOM can impart a negative
759 surface charge and steric forces among particles in aquatic systems, which subsequently improves the

760 stability of PS MPs and PSNPs-COOH in the absence of electrolytes (Li et al., 2018; Wu et al., 2019a).
761 HA and fulvic acids (FA) are main fractions of DOM, and are often used as a model DOM (Cai et al.,
762 2018). In ultrapure water, high concentration of HA ($30 \text{ mg}\cdot\text{L}^{-1}$) induced the aggregation of PSNPs-
763 NH_2 with positive charges because the addition of HA significantly (ANOVA, $F= 1497$, $p < 0.001$)
764 decreased the zeta potential (from $> 50 \text{ mV}$ to 24.3 mV) (Tallec et al., 2019). No aggregation of PSNPs-
765 NH_2 was observed at low concentration of HA (1 and $10 \text{ mg}\cdot\text{L}^{-1}$) due to the insufficient neutralization
766 effect.

767 The electrolyte valence played important roles in the aggregation of MPs in DOM (i.e., HA and
768 FA) (Singh et al., 2019). In monovalent electrolyte solutions, DOM provided steric hindrance forces
769 and electrostatic repulsion to stabilize PS NPs and PSNPs-COOH (Yu et al., 2019). Both HA and FA
770 had negligible effects on the aggregation of negatively charged PS NPs in NaCl solution due to high
771 electrostatic repulsive forces between particles (Cai et al., 2018). HA in the concentration range of 0 -
772 $50 \text{ mg}\cdot\text{L}^{-1}$ promoted the aggregation of positively charged PSNPs- NH_2 in NaCl solution owing to the
773 charge neutralization effect (Wu et al., 2019a). In the presence of divalent or trivalent metal ions,
774 DOM destabilized MPs through the bridge attraction and intermolecular bridging between metal ions
775 and surface functional groups of DOM (Li et al., 2018). For example, in CaCl_2 solution, DOM at low-
776 concentration ($< 5 \text{ mg}\cdot\text{C}\cdot\text{L}^{-1}$) inhibited the aggregation of PS NPs through steric repulsion, but
777 accelerated the aggregation at high DOM concentrations ($> 5 \text{ mg}\cdot\text{C}\cdot\text{L}^{-1}$) through the complexation
778 between Ca^{2+} and carboxyl groups of DOM (Singh et al., 2019; Yu et al., 2019). Similarly, in 1 mM
779 FeCl_3 solution, the complexation reaction between Fe^{3+} and carboxyl groups of DOM (i.e., HA and FA)
780 adsorbed on PS NP surfaces decreased their stability (Cai et al., 2018).

781 In the mixture of artificial seawater and HA, the hydrodynamic diameters of PSNPs-COOH and
782 PS NPs increased significantly ($p < 0.001$) with sizes exceeding $1 \mu\text{m}$ in 24 h due to the charge
783 neutralization effect of divalent cations and bridging effect (Tallec et al., 2019). However, HA

784 significantly decreased the hydrodynamic diameters of PS NPs ($p < 0.001$) in artificial seawater in 24
785 h to 48 h, causing a stabilizing effect and partial disaggregation presumably due to the increase of
786 steric repulsion forces (Qu et al., 2010). In freshwater, high concentration of nature organic matter,
787 such as alginate and HA, can alleviate the toxicity to zooplankton through increasing stability of MPs
788 or forming an eco-corona on MP surface (Saavedra et al., 2019; Wu et al., 2019a).

789 **4.2.4 Effect of surfactant**

790 Surfactants are widely used in domestic and industrial products, and they are frequently used
791 reagents to disperse MPs in water (Skaf et al., 2020). Electrostatic repulsion played a dominant role in
792 increasing colloidal stability, and thereby varying aggregation rates when ionic surfactants covered
793 MPs (Jódar-Reyes et al., 2006b). A cationic surfactant, domiphen bromide, resulted in the aggregation
794 of negatively charged PSNPs-COOH particles due to the charge neutralization effect (Jódar-Reyes et
795 al., 2006b). Similarly, an anionic surfactant, sodium dodecylbenzenesulfonate, promoted the
796 aggregation of positively charged amphoteric PS MPs (diameter around 350 nm). In both the above
797 cases, electrostatic repulsion forces were reduced among the plastic particles due to the presence of
798 surfactant molecules (Jódar-Reyes et al., 2006b). Additionally, the adsorption of non-ionic surfactants
799 on latex particles at high surface coverage could act as a steric stabilizer, and thus improve the stability
800 of PS MPs (Romero-Cano et al., 2000).

801 **4.2.5 Effect of light**

802 Solar irradiation, especially the UVA fraction of sunlight, was found to change the
803 physicochemical properties (surface polarity and functional groups) of NPs and alter their aggregation
804 behavior in water (Liu et al., 2019b). The stability of PS NPs was improved in NaCl solution but
805 decreased in CaCl₂ solution after exposure to UV light. The high stability of PS NPs in NaCl solution
806 was likely because of the following three reasons: (1) lowered van der Waals attraction between aged
807 PS NPs because of their decreased Hamaker constants; (2) increased electrostatic forces due to

808 deprotonation of oxygen-containing functional groups generated on aged PS NPs; and (3) enhanced
809 steric hindrance forces between UV-exposed PS NPs rendered by the leaching organic matter (Liu et
810 al., 2019b). The aggregation of PS NPs was promoted in CaCl₂ solution primarily because Ca²⁺ could
811 complex with oxygen-containing functional groups such as carbonyl and carboxyl groups, that were
812 formed on UV-irradiated PS NP surfaces (Qu et al., 2010).

813 **4.3. Other factors**

814 Microorganisms, phytoplankton and suspended sediments widely existing in natural waters can
815 remarkably interfere with the aggregation states of MPs (Long et al., 2015; Zhang and Chen, 2019).
816 The negatively charged algae *Chlorella sp.* was found to form heteroaggregates with positively
817 charged PSNPs-NH₂ particles but not with negatively charged PSNPs-COOH (Thiagarajan et al.,
818 2019). Cellulose is a component of the cell wall of many algal species such as *Chlorella* and
819 *Scenedesmus* (Bhattacharya et al., 2010). If suspended in water, cellulose can initiate
820 heteroaggregation between algal cells and MPs. Similarly, EPS enhanced the heteroaggregation of PS
821 MPs and PVC MPs with *Chlorella pyrenoidosa* and *Skeletonema costatum* cells (Mao et al., 2018;
822 Zhang et al., 2017). In addition to microorganisms, Li et al. (2019) indicated that suspended sediment
823 formed heteroaggregates with PS NPs and promoted settling of plastic particles in NaCl solution.
824 However, the interaction between PE MPs and suspended sediments was minor, and PE MPs floated
825 on the water surface for 8 months after the addition of 500 mg·L⁻¹ suspended sediments.

826 **5. Environmental implications of MP aggregation**

827 Investigating the aggregation behavior of MPs is of great importance to elucidate their potential
828 environmental implications after their release into natural waters (Rummel et al., 2017). Significant
829 consequences concerning the aggregation of MPs are their altered particle sizes and specific surface
830 areas, which subsequently impact their toxicity toward organisms, their own transformations, co-
831 transport with other pollutants, and formation of biofilm.

832 **5.1 Transport and transformation of microplastics**

833 The aggregation of MPs determines their distribution in natural waters (Bhattacharya et al., 2010).
834 Nano- and micro-sized particulate plastics floating on the water surface can form aggregates with
835 microbial communities or plankton, which may affect the density of the plastics and change their depth
836 in natural waters (Alimi et al., 2018). Aggregates of MPs located at different water depths undergo
837 different degrees of weathering from solar irradiation, biological degradation, mechanical wearing,
838 and pyrolysis, which results in different mass losses or degradation rates of the plastic aggregates
839 (Alimi et al., 2018). Solar irradiation plays a primary role in the photodegradation and pyrolysis of
840 plastic aggregates in the upper surface of natural waters (Chatani et al., 2014). The plastic aggregates
841 can absorb sunlight and generate free radicals through impurities, which lead MPs to break into small
842 fragments with low molecular weights (Zhao et al., 2018). Plastic aggregates settling to the seabed are
843 not affected by illumination, but the complex hydrodynamic processes and microorganisms
844 significantly affect the physicochemical properties and fates of the bottom plastic aggregates (Zhao et
845 al., 2018).

846 **5.2 Toxicity to organisms**

847 The toxicity of MPs to organisms depends on their aggregate size (Fan et al., 2019). The
848 aggregated MPs could be less bioavailable to aquatic organisms because the toxicity of particles was
849 inversely proportional to size in general (Choi et al., 2019). In natural seawater, PSNPs-NH₂ formed
850 nano-sized aggregates (< 200 nm) inducing death of brine shrimps in 14 d (LC₅₀ = 0.83 µg·mL⁻¹) and
851 inhibition of algal growth (EC₅₀ = 12.97 µg·mL⁻¹) (Bergami et al., 2017). By contrast, PSNPs-COOH
852 rapidly formed micro-sized aggregates (> 1 µm), thereby greatly reduced the toxicity to brine shrimps
853 (LC₅₀ > 10 µg·mL⁻¹) or microalgae (EC₅₀ > 50 µg·mL⁻¹). It should be noted that MP aggregates outside
854 the organisms could exert negative effect (Wu et al., 2019a; Zhu et al., 2019). For instance, MP
855 aggregates inhibited the photosynthesis process and limited the transfer of nutriment and energy of

856 microalgae in marine ecosystem (Zhu et al., 2019). In addition, the MP-biota heteroaggregates could
857 cause physical damage such as split and oxidative stress toward organisms (Choi et al., 2019; Zhu et
858 al., 2019). The positively charged PS NPs were more prone to aggregate with marine bacterium
859 (*Halomonas alkaliphile*) via electrostatic attraction, which induced higher toxicity than negatively
860 charged PS NPs (Sun et al., 2018).

861 The aggregate dimensions of MPs in natural waters fall in the range from nanometers to
862 centimeters or larger, and this could lead to their toxicity toward organisms in different layers of water
863 column (Browne et al., 2008; Ward and Kach, 2009). If MPs aggregated slightly, Brownian motion
864 can keep them suspended on the water surface for months or even longer (Li et al., 2019). The
865 suspended or floated plastic aggregates pose negative effect on zooplankton, planktivory, filter feeders
866 or suspension-feeders. Plastic particles with a large degree of aggregation settle quickly and
867 accumulate in the seabed and sediments (Bergami et al., 2017). Colonization of MPs with organisms
868 results in their higher densities and sinking to the benthos (Galloway et al., 2017). They eventually
869 exert toxic effect on deposit feeders and detritivores that inhabit in the seabed. Because many toxic
870 pollutants could be adsorbed on the surface of sinking plastic aggregates, the detoxification effect for
871 organisms living in the water surface could occur, but toxic effects would transfer to the benthic
872 organisms (Zhang et al., 2017).

873 The regional variation in biotoxicity of MPs can be assessed by toxicity assay of organisms
874 exposed to MPs in the laboratory through three steps (Bergami et al., 2017; Saavedra et al., 2019).
875 First, water samples or aquatic organisms from different layers of natural waters are collected (de Sá
876 et al., 2018). Second, the type, shape, size and concentration of MPs in those field samples are analyzed
877 (Nan et al., 2020). Third, MPs collected in the field or pristine MPs having similar physicochemical
878 properties with those in the field are selected to examine the ecotoxicity of MPs toward model
879 organisms in the laboratory (Sendra et al., 2019; Zhu et al., 2019). In general, the most frequently

880 applied model organisms include planktonic crustacean (*Daphnia magna*) as zooplankton, fish (*Danio*
881 *rerio* and *Pomatoschistus microps*) as organisms in water column, and mollusc (blue mussel *M. edulis*)
882 as benthic organisms (de Sá et al., 2018).

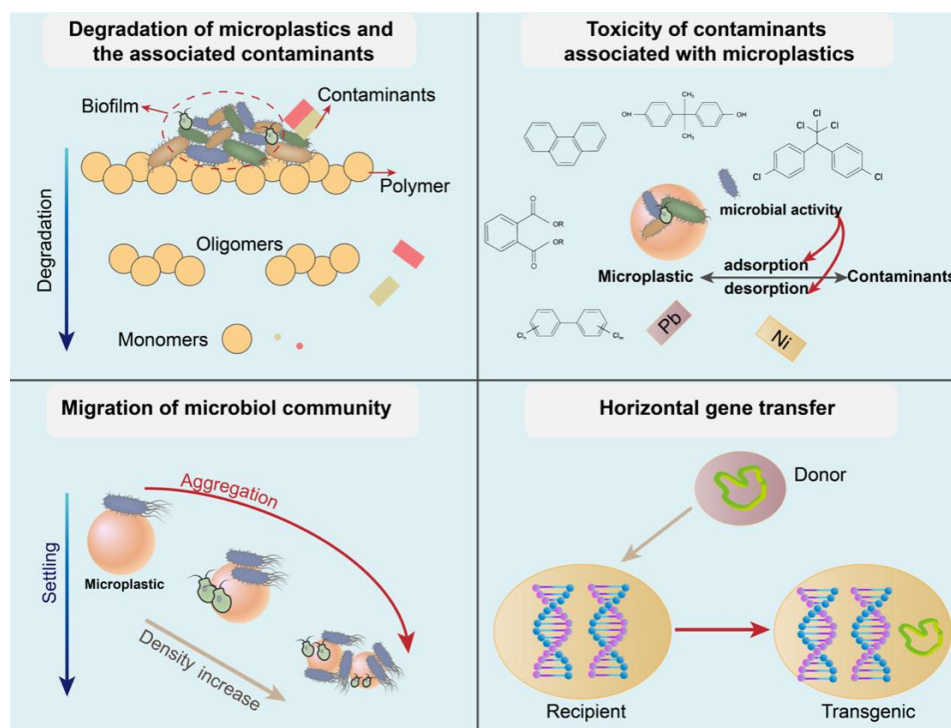
883 **5.3 Transport of contaminants**

884 MPs can transport pollutants in the following two ways. Firstly, the additives, monomers, and
885 non-intentionally added substances (e.g., flame retardants, phthalate, plasticizers and heavy metals)
886 can be leached by MPs (Suhrhoﬀ and Scholz-Böttcher, 2016; Xu et al., 2020). Some of these
887 contaminants are extremely harmful toward organisms (Suhrhoﬀ and Scholz-Böttcher, 2016).
888 Secondly, MPs may act as a transport vector for organic pollutants and heavy metals because MPs
889 may adsorb these pollutants on their surfaces (Cole et al., 2011). Aggregation of MPs may alter their
890 particle sizes and surface areas, which is a key factor determining the transport of the released additives
891 and the adsorbed contaminants (Yang et al., 2018). Compared to large aggregates, small aggregates of
892 MPs with larger surface areas and more reactive sites may release more contaminants and degrade
893 faster (Chen et al., 2019). For example, organotin compounds (dimethyltin and dibutyltin) were
894 released from PVC MPs under UV and visible light irradiation, and the released content of organotin
895 by small sized PVC MPs (10 µm) was nearly 1000-fold higher than that by large sized PVC MPs (300
896 µm) after 56-h UV or visible light irradiation (Chen et al., 2019).

897 **5.4 Microbial habitation and biofilm formation**

898 Plastic surfaces exhibit hydrophobicity that facilitates DOM adsorption in aquatic ecosystems.
899 Biofilms of microorganisms can then form on plastic surfaces due to abundant carbon and nutrient
900 sources in the DOM (Harrison et al., 2018). Microbial habitation of MPs and subsequent biofilm
901 formation facilitates the aggregation of MPs, which has several implications that include (**Fig. 5**): (1)
902 degradation of MPs and the associated contaminants; (2) horizontal gene transfer between
903 microorganisms; (3) toxicity of contaminants associated with MPs; and (4) migration or spreading of

904 microorganisms especially in aquatic ecosystems (Oberbeckmann et al., 2015; Rummel et al., 2017).
 905 Biodegradation of MPs and consequent release of associated organic contaminants are accelerated by
 906 certain organisms present in the biofilm. Moreover, there is growing evidence that the microbial
 907 habitation in the biofilm can promote gene exchange (Jacquin et al., 2019); so determining the
 908 potential of biofilms for providing the surface for anti-microbial resistance gene transfer is important.
 909 Adsorption and desorption processes of pollutants on MP surface in water are influenced by factors
 910 such as microbial activity, MP weathering and surface area, and interaction with DOM. MPs provide
 911 a more robust vehicle than biodegradable biotic substrates for the transport of organisms over long
 912 distances, which can facilitate the movement of microorganisms to different ecosystems and
 913 potentially introduce invasive and exotic species (Viršek et al., 2017).



914
 915 **Fig. 5.** Implications of microbial habitation and biofilm formation on microplastics.

916 **5.5 Environmental management**

917 The wide distribution and ecological risk of MPs in aquatic environment are a symptom of
 918 mismanagement of plastic wastes, particularly MP debris (Karbalaei et al., 2018). Despite the policies

919 and regulations in many countries are implemented to reduce the risk of MPs, the action plans have
920 not considered the potential impacts resulting from the aggregation behaviors of MPs (Auta et al.,
921 2017; Praetorius et al., 2020). In addition, studies have not been conducted extensively on MP
922 aggregation in the field (Li et al., 2019). Therefore it is imperative to investigate the aggregation of
923 MPs in environmentally relevant conditions and/or in the field. On the other hand, the need for MP
924 cleaning-up strategy should be considered. Based on systematic investigations of MP aggregation, the
925 removal efficiency of MPs in WWTPs and drinking water treatment via flocculation processes can be
926 promoted (Skaf et al., 2020; Zhang and Chen, 2019). Studies have shown that MP surfaces are suitable
927 substrates for microbial growth, thus biodegradation can be harnessed to degrade MPs (Auta et al.,
928 2017). Manufacturers are encouraged to produce plastics with biodegradable materials (Gallo et al.,
929 2018).

930 **6. Knowledge gaps and future recommendations**

931 From numerous studies concerning MPs in the environment, it is evident that although our
932 understanding of MP aggregation in water environments is advancing, currently no standard methods
933 exist for MP separation and identification. Similarly, studies concerning the mobility of MPs in real
934 environments are far from fully understood. To fill these knowledge gaps and fully reveal the
935 influences of plastic pollution on the environment, following most important research issues deserve
936 immediate attention:

937 **6.1 More field studies**

938 Most published works focused on the investigations of stability and mobility of MPs in laboratory
939 scales with only a few works studying the aggregation of MPs in environmentally relevant systems,
940 especially in natural surface waters, groundwater, or WWTPs. The natural water system is complex
941 and contains DOM, microorganisms, mixtures of contaminants, and the laboratory research using
942 simulated natural waters may misestimate MPs aggregation behaviors. There is an urgent need to study

943 the homoaggregation and heteroaggregation behaviors of primary and secondary MPs in the field to
944 understand how UV weathering and biological processes impact the stability of MPs in natural waters.
945 In addition, river sediments are important sinks for MPs. Further work is therefore needed to better
946 understand the aggregation of MPs in these complex heterogeneous media. Most of the laboratory
947 aggregation studies have been conducted over one hour, but this only provides an initial snapshot of
948 the aggregate. Therefore, it is necessary to perform temporal stability experiments which would allow
949 to evaluate long-term impact of MPs.

950 **6.2 Use microplastics in laboratory works representing those in the environment**

951 Notably, the majority of existing laboratory studies on the aggregation of MPs have used
952 commercial and spherical PS particles with sulfate, amine or carboxyl groups, which are less likely to
953 exist in natural waters (Wang et al., 2020). Most MPs in the environment are expected to have non-
954 spherical shapes (e.g., fibers, strings, pellets, films, thin sheets) and varying compositions (e.g., PE,
955 PP, PVC, polyethylene terephthalate). Therefore, future aggregation research should consider the
956 diversity of MPs to better elucidate their mobility and associated behaviors. In addition, the
957 aggregation behaviors of environmentally relevant secondary MPs comprised of fragments, fibers,
958 films, and rods warrant further examination. Many previous studies on the aggregation of MPs in water
959 have applied extremely high doses of MPs which do not reflect real-world conditions, and resulted in
960 misinterpretation of the results. Researchers are suggested to use environmentally realistic
961 concentration of MPs to yield more realistic estimates of MPs' impacts in aquatic environments.

962 **6.3 Standardization of identification and quantification methods**

963 Visual observation is one of the most frequently used techniques for distinguishing between the
964 homoaggregation and heteroaggregation with other solid constituents in water. However, nearly 70%
965 of small particles, which are characterized visually as MPs, are not confirmed as plastics by chemical
966 detection methods. Therefore, the spectroscopic techniques such as EDS, FTIR, Raman spectroscopy

967 are strongly recommended to combine with visual observations for a reliable characterization of MP
968 stability in water environments. In addition, the commonly applied visual observations are insufficient
969 to investigate the aggregation of MPs in environmental samples. Small-sized MPs, especially for the
970 case of MPs <500 μm size, remain poorly understood because of the limitations of existing detection
971 methods and their low resolution for particles at nanoscale. Because the standardized methods for
972 sample collection, identification, and quantification are still in their infancy, comparison of results
973 among different works becomes difficult. Therefore, new research methods should be carefully
974 collated together to formulate standard protocols.

975 **Declaration of Competing Interest**

976 The authors declare that they have no known competing financial interests or personal
977 relationships that could have appeared to influence the work reported in this paper.

978 **Acknowledgements**

979 This study was financially supported by the National Natural Science Foundation of China (grant
980 number 21677015) and Hong Kong Research Grants Council (E-PolyU503/17).

981 **References**

- 982 Adan, A., Alizada, G., Kiraz, Y., Baran, Y., Nalbant, A., 2017. Flow cytometry: Basic principles and applications. *Crit. Rev.*
983 *Biotechnol.* 37, 163-176.
- 984 Alimi, O.S., Budarz, J.F., Hernandez, L.M., Tufenkji, N., 2018. Microplastics and nanoplastics in aquatic environments:
985 Aggregation, deposition, and enhanced contaminant transport. *Environ. Sci. Technol.* 52, 1704-1724.
- 986 Anderson, J.C., Park, B.J., Palace, V.P., 2016. Microplastics in aquatic environments: Implications for Canadian
987 ecosystems. *Environ. Pollut.* 218, 269-280.
- 988 Anderson, P.J., Warrack, S., Langen, V., Challis, J.K., Hanson, M.L., Rennie, M.D., 2017. Microplastic contamination in
989 Lake Winnipeg, Canada. *Environ. Pollut.* 225, 223-231.
- 990 Andrady, A.L., 2011. Microplastics in the marine environment. *Mar. Pollut. Bull.* 62, 1596-1605.
- 991 Arias-Andres, M., Klumper, U., Rojas-Jimenez, K., Grossart, H.P., 2018. Microplastic pollution increases gene exchange
992 in aquatic ecosystems. *Environ. Pollut.* 237, 253-261.
- 993 Auta, H.S., Emenike, C.U., Fauziah, S.H., 2017. Distribution and importance of microplastics in the marine environment:
994 A review of the sources, fate, effects, and potential solutions. *Environ. Int.* 102, 165-176.
- 995 Bähler, M., Nguyen, T.H., Tang, F.H.M., Maggi, F., 2020. Sinking of microbial-associated microplastics in natural waters.

996 Plos One 15, 1-20.

997 Bergami, E., Pugnali, S., Vannuccini, M.L., Manfra, L., Faleri, C., Savorelli, F., Dawson, K.A., Corsi, I., 2017. Long-
998 term toxicity of surface-charged polystyrene nanoplastics to marine planktonic species *Dunaliella tertiolecta* and *Artemia*
999 *franciscana*. *Aquat. Toxicol.* 189, 159-169.

1000 Bergmann, M., Mützel, S., Pimpke, S., Tekman, M.B., Trachsel, J., Gerdt, G., 2019. White and wonderful? Microplastics
1001 prevail in snow from the Alps to the Arctic. *Sci. Adv.* 5, eaax1157.

1002 Bhattacharya, P., Lin, S., Turner, J.P., Ke, P.C., 2010. Physical adsorption of charged plastic nanoparticles affects algal
1003 photosynthesis. *J. Phys. Chem. C* 114, 16556-16561.

1004 Blom, M.T., Chmela, E., Oosterbroek, R.E., Tijssen, R., Van Den Berg, A., 2003. On-chip hydrodynamic chromatography
1005 separation and detection of nanoparticles and biomolecules. *Anal. Chem.* 75, 6761-6768.

1006 Bolan, N.S., Naidu, R., Syers, J.K., Tillman, R.W., 1999. Surface charge and solute interactions in soils. *Adv. Agron.* 67,
1007 87-140.

1008 Bouwmeester, H., Hollman, P.C., Peters, R.J., 2015. Potential health impact of environmentally released micro-and
1009 nanoplastics in the human food production chain: Experiences from nanotoxicology. *Environ. Sci. Technol.* 49, 8932-8947.

1010 Browne, M.A., Dissanayake, A., Galloway, T.S., Lowe, D.M., Thompson, R.C., 2008. Ingested microscopic plastic
1011 translocates to the circulatory system of the mussel, *mytilus edulis* (L.). *Environ. Sci. Technol.* 42, 5026-5031.

1012 Cai, L., Hu, L., Shi, H., Ye, J., Zhang, Y., Kim, H., 2018. Effects of inorganic ions and natural organic matter on the
1013 aggregation of nanoplastics. *Chemosphere* 197, 142-151.

1014 Campanale, C., Stock, F., Massarelli, C., Kochleus, C., Bagnuolo, G., Reifferscheid, G., Uricchio, V.F., 2020. Microplastics
1015 and their possible sources: The example of Ofanto river in southeast Italy. *Environ. Pollut.* 258, 113284.

1016 Capolupo, M., Sorensen, L., Jayasena, K.D.R., Booth, A.M., Fabbri, E., 2020. Chemical composition and ecotoxicity of
1017 plastic and car tire rubber leachates to aquatic organisms. *Water Res.* 169, 115270.

1018 Castelvetro, V., Corti, A., Bianchi, S., Ceccarini, A., Manariti, A., Vinciguerra, V., 2020. Quantification of poly(ethylene
1019 terephthalate) micro- and nanoparticle contaminants in marine sediments and other environmental matrices. *J. Hazard.*
1020 *Mater.* 385, 121517.

1021 Cejas, C.M., Monti, F., Truchet, M., Burnouf, J.-P., Tabeling, P., 2018. Universal diagram for the kinetics of particle
1022 deposition in microchannels. *Phys. Rev. E* 98, 062606.

1023 EFSA CONTAM Panel (EFSA Panel on Contaminants in the Food Chain), 2016. Presence of microplastics and
1024 nanoplastics in food, with particular focus on seafood. *EFSA Journal* 14, 4501-4531.

1025 Chamas, A., Moon, H., Zheng, J., Qiu, Y., Tabassum, T., Jang, J.H., Abu-Omar, M., Scott, S.L., Suh, S., 2020. Degradation
1026 rates of plastics in the environment. *ACS Sustain. Chem. Eng.* 8, 3494-3511.

1027 Chatani, S., Kloxin, C.J., Bowman, C.N., 2014. The power of light in polymer science: Photochemical processes to
1028 manipulate polymer formation, structure, and properties. *Polym. Chem-UK.* 5, 2187-2201.

1029 Chen, C., Chen, L., Yao, Y., Artigas, F., Huang, Q., Zhang, W., 2019. Organotin release from polyvinyl chloride
1030 microplastics and concurrent photodegradation in water: Impacts from salinity, dissolved organic matter, and light exposure.
1031 *Environ. Sci. Technol.* 53, 10741-10752.

1032 Choi, J.S., Hong, S.H., Park, J.W., 2019. Evaluation of microplastic toxicity in accordance with different sizes and exposure
1033 times in the marine copepod *Tigriopus japonicus*. *Mar. Environ. Res.*, 104838.

1034 Chowdhury, I., Duch, M.C., Mansukhani, N.D., Hersam, M.C., Bouchard, D., 2013. Colloidal properties and stability of
1035 graphene oxide nanomaterials in the aquatic environment. *Environ. Sci. Technol.* 47, 6288-6296.

1036 Cincinelli, A., Scopetani, C., Chelazzi, D., Lombardini, E., Martellini, T., Katsoyiannis, A., Fossi, M.C., Corsolini, S.,
1037 2017. Microplastic in the surface waters of the Ross Sea (Antarctica): Occurrence, distribution and characterization by

1038 FTIR. Chemosphere 175, 391-400.

1039 Cole, M., Lindeque, P., Halsband, C., Galloway, T.S., 2011. Microplastics as contaminants in the marine environment: A
1040 review. Mar. Pollut. Bull. 62, 2588-2597.

1041 Correia, M., Loeschner, K., 2018. Detection of nanoplastics in food by asymmetric flow field-flow fractionation coupled
1042 to multi-angle light scattering: Possibilities, challenges and analytical limitations. Anal. Bioanal. Chem. 410, 5603-5615.

1043 Cunha, C., Faria, M., Nogueira, N., Ferreira, A., Cordeiro, N., 2019. Marine vs freshwater microalgae exopolymers as
1044 biosolutions to microplastics pollution. Environ. Pollut. 249, 372-380.

1045 Cutroneo, L., Reboa, A., Besio, G., Borgogno, F., Canesi, L., Canuto, S., Dara, M., Enrile, F., Forioso, I., Greco, G., 2020.
1046 Microplastics in seawater: Sampling strategies, laboratory methodologies, and identification techniques applied to port
1047 environment. Environ. Sci. Pollut. R. 27, 8938-8952.

1048 de Sá, L.C., Oliveira, M., Ribeiro, F., Rocha, T.L., Futter, M.N., 2018. Studies of the effects of microplastics on aquatic
1049 organisms: What do we know and where should we focus our efforts in the future? Sci. Total. Environ. 645, 1029-1039.

1050 Dong, Z., Qiu, Y., Zhang, W., Yang, Z., Wei, L., 2018. Size-dependent transport and retention of micron-sized plastic
1051 spheres in natural sand saturated with seawater. Water Res. 143, 518-526.

1052 Dris, R., Gasperi, J., Saad, M., Mirande, C., Tassin, B., 2016. Synthetic fibers in atmospheric fallout: A source of
1053 microplastics in the environment? Mar. Pollut. Bull. 104, 290-293.

1054 Duis, K., Coors, A., 2016. Microplastics in the aquatic and terrestrial environment: Sources (with a specific focus on
1055 personal care products), fate and effects. Environ. Sci. Eur. 28, 2.

1056 Edo, C., González-Pleiter, M., Leganés, F., Fernández-Piñas, F., Rosal, R., 2020. Fate of microplastics in wastewater
1057 treatment plants and their environmental dispersion with effluent and sludge. Environ. Pollut. 259, 113837.

1058 Eerkes-Medrano, D., Thompson, R.C., Aldridge, D.C., 2015. Microplastics in freshwater systems: A review of the
1059 emerging threats, identification of knowledge gaps and prioritisation of research needs. Water Res. 75, 63-82.

1060 Efimova, I., Bagaeva, M., Bagaev, A., Kileso, A., Chubarenko, I.P., 2018. Secondary microplastics generation in the sea
1061 swash zone with coarse bottom sediments: Laboratory experiments. Front. Mar. Sci. 5, 313.

1062 Eo, S., Hong, S.H., Song, Y.K., Han, G.M., Shim, W.J., 2019. Spatiotemporal distribution and annual load of microplastics
1063 in the Nakdong River, South Korea. Water Res. 160, 228-237.

1064 Estahbanati, S., Fahrenfeld, N.L., 2016. Influence of wastewater treatment plant discharges on microplastic concentrations
1065 in surface water. Chemosphere 162, 277-284.

1066 Fan, Z., Zhuang, W., Se, W., Hao, F., Degao, W., 2019. Aquatic behavior and toxicity of polystyrene nanoplastic particles
1067 with different functional groups: Complex roles of pH, dissolved organic carbon and divalent cations. Chemosphere 228,
1068 195-203.

1069 Fendall, L.S., Sewell, M.A., 2009. Contributing to marine pollution by washing your face: Microplastics in facial cleansers.
1070 Mar. Pollut. Bull. 58, 1225-1228.

1071 Feng, L.J., Sun, X.D., Zhu, F.P., 2020. Nanoplastics promote microcystin synthesis and release from cyanobacterial
1072 *Microcystis aeruginosa*. Environ. Sci. Technol. 54, 3386-3394.

1073 Fischer, E.K., Paglialonga, L., Czech, E., Tamminga, M., 2016. Microplastic pollution in lakes and lake shoreline sediments
1074 - A case study on Lake Bolsena and Lake Chiusi (central Italy). Environ. Pollut. 213, 648-657.

1075 Fraunhofer, W., Winter, G., Coester, C., 2004. Asymmetrical flow field-flow fractionation and multiangle light scattering
1076 for analysis of gelatin nanoparticle drug carrier systems. Anal. Chem. 76, 1909-1920.

1077 Fu, W., Min, J., Jiang, W., Li, Y., Zhang, W., 2020. Separation, characterization and identification of microplastics and
1078 nanoplastics in the environment. Sci. Total Environ. 721, 137561.

1079 Fu, W., Zhang, W., 2018. Measurement of the surface hydrophobicity of engineered nanoparticles using an atomic force

1080 microscope. *Phys. Chem. Chem. Phys.* 20, 24434-24443.

1081 Galafassi, S., Nizzetto, L., Volta, P., 2019. Plastic sources: A survey across scientific and grey literature for their inventory
1082 and relative contribution to microplastics pollution in natural environments, with an emphasis on surface water. *Sci. Total.*
1083 *Environ.* 693, 133499.

1084 Gallo, F., Fossi, C., Weber, R., Santillo, D., Sousa, J., Ingram, I., Nadal, A., Romano, D., 2018. Marine litter plastics and
1085 microplastics and their toxic chemicals components: The need for urgent preventive measures. *Environ. Sci. Eur.* 30, 13.

1086 Galloway, T.S., Cole, M., Lewis, C., 2017. Interactions of microplastic debris throughout the marine ecosystem. *Nat. Ecol.*
1087 *Evol.* 1, 1-8.

1088 Gigault, J., El Hadri, H., Reynaud, S., Deniau, E., Grassl, B., 2017. Asymmetrical flow field flow fractionation methods
1089 to characterize submicron particles: Application to carbon-based aggregates and nanoplastics. *Anal. Bioanal. Chem.* 409,
1090 6761-6769.

1091 Gigault, J., Halle, A.T., Baudrimont, M., Pascal, P.Y., Gauffre, F., Phi, T.L., El Hadri, H., Grassl, B., Reynaud, S., 2018.
1092 Current opinion: What is a nanoplastic? *Environ. Pollut.* 235, 1030-1034.

1093 Gigault, J., Pedrono, B., Maxit, B., Ter Halle, A., 2016. Marine plastic litter: The unanalyzed nano-fraction. *Environmental*
1094 *Science: Nano* 3, 346-350.

1095 Green, R.E., Sosik, H.M., Olson, R.J., DuRand, M.D., 2003. Flow cytometric determination of size and complex refractive
1096 index for marine particles: Comparison with independent and bulk estimates. *Appl. Optics* 42, 526-541.

1097 Gross, J., Sayle, S., Karow, A.R., Bakowsky, U., Garidel, P., 2016. Nanoparticle tracking analysis of particle size and
1098 concentration detection in suspensions of polymer and protein samples: Influence of experimental and data evaluation
1099 parameters. *Eur. J. Pharm. Biopharm.* 104, 30-41.

1100 Guerranti, C., Martellini, T., Perra, G., Scopetani, C., Cincinelli, A., 2019. Microplastics in cosmetics: Environmental
1101 issues and needs for global bans. *Environ. Toxicol. Pharmacol.* 68, 75-79.

1102 Hale, R.C., 2017. Analytical challenges associated with the determination of microplastics in the environment. *Anal.*
1103 *Methods-UK* 9, 1326-1327.

1104 Harrison, J.P., Hoellein, T.J., Sapp, M., Tagg, A.S., Ju-Nam, Y., Ojeda, J.J. 2018. Microplastic-associated biofilms: a
1105 comparison of freshwater and marine environments. *Freshwater microplastics*. Springer, pp. 181-201.

1106 He, Y., Wan, J., Tokunaga, T., 2008. Kinetic stability of hematite nanoparticles: The effect of particle sizes. *J. Nanopart.*
1107 *Res.* 10, 321-332.

1108 Hidalgo-Ruz, V., Gutow, L., Thompson, R.C., Thiel, M., 2012. Microplastics in the marine environment: A review of the
1109 methods used for identification and quantification. *Environ. Sci. Technol.* 46, 3060-3075.

1110 Hierrezuelo, J., Sadeghpour, A., Szilagy, I., Vaccaro, A., Borkovec, M., 2010. Electrostatic stabilization of charged
1111 colloidal particles with adsorbed polyelectrolytes of opposite charge. *Langmuir* 26, 15109-15111.

1112 Huffer, T., Praetorius, A., Wagner, S., von der Kammer, F., Hofmann, T., 2017. Microplastic exposure assessment in aquatic
1113 environments: Learning from similarities and differences to engineered nanoparticles. *Environ. Sci. Technol.* 51, 2499-
1114 2507.

1115 Huppertsberg, S., Knepper, T.P., 2018. Instrumental analysis of microplastics-benefits and challenges. *Anal. Bioanal. Chem.*
1116 410, 6343-6353.

1117 Jacquin, J., Cheng, J., Odobel, C., Conan, P., Pujo-pay, M., Jean-Francois, G., 2019. Microbial ecotoxicology of marine
1118 plastic debris: A review on colonization and biodegradation by the 'plastisphere'. *Front. microbiol.* 10, 865.

1119 Jódar-Reyes, A.B., Martín-Rodríguez, A., Ortega-Vinuesa, J.L., 2006a. Effect of the ionic surfactant concentration on the
1120 stabilization/destabilization of polystyrene colloidal particles. *J. Colloid Interf. Sci.* 298, 248-257.

1121 Jódar-Reyes, A.B., Ortega-Vinuesa, J.L., Martín-Rodríguez, A., 2006b. Electrokinetic behavior and colloidal stability of

1122 polystyrene latex coated with ionic surfactants. *J. Colloid Interf. Sci.* 297, 170-181.

1123 Kaberova, Z., Karpushkin, E., Nevoralova, M., Vetric, M., Slouf, M., Duskova-Smrckova, M., 2020. Microscopic structure
1124 of swollen hydrogels by scanning electron and light microscopies: Artifacts and reality. *Polymers-Basel* 12, 578.

1125 Karbalaei, S., Hanachi, P., Walker, T.R., Cole, M., 2018. Occurrence, sources, human health impacts and mitigation of
1126 microplastic pollution. *Environ. Sci. Pollut. Res. Int.* 25, 36046-36063.

1127 Kastner, E., Perrie, Y. 2016. Particle Size Analysis of Micro and Nanoparticles. *Analytical Techniques in the*
1128 *Pharmaceutical Sciences*. Springer, pp. 677-699.

1129 Kaszuba, M., Corbett, J., Watson, F.M., Jones, A., 2010. High-concentration zeta potential measurements using light-
1130 scattering techniques. *Philos. T. R. Soc. A.* 368, 4439-4451.

1131 Kataoka, T., Nihei, Y., Kudou, K., Hinata, H., 2019. Assessment of the sources and inflow processes of microplastics in
1132 the river environments of Japan. *Environ. Pollut.* 244, 958-965.

1133 Kazour, M., Terki, S., Rabhi, K., Jemaa, S., Khalaf, G., Amara, R., 2019. Sources of microplastics pollution in the marine
1134 environment: Importance of wastewater treatment plant and coastal landfill. *Mar. Pollut. Bull.* 146, 608-618.

1135 Klang, V., Matsko, N.B., Valenta, C., Hofer, F., 2012. Electron microscopy of nanoemulsions: An essential tool for
1136 characterisation and stability assessment. *Micron.* 43, 85-103.

1137 Kumari, A., Chaudhary, D.R., Jha, B., 2018. Destabilization of polyethylene and polyvinylchloride structure by marine
1138 bacterial strain. *Environ. Sci. Pollut. R.* 26, 1507-1516.

1139 Lagarde, F., Olivier, O., Zanella, M., Daniel, P., Hiard, S., Caruso, A., 2016. Microplastic interactions with freshwater
1140 microalgae: Hetero-aggregation and changes in plastic density appear strongly dependent on polymer type. *Environ. Pollut.*
1141 215, 331-339.

1142 Lambert, S., Wagner, M., 2016. Characterisation of nanoplastics during the degradation of polystyrene. *Chemosphere* 145,
1143 265-268.

1144 Lei, K., Qiao, F., Liu, Q., Wei, Z., Qi, H., Cui, S., Yue, X., Deng, Y., An, L., 2017. Microplastics releasing from personal
1145 care and cosmetic products in China. *Mar. Pollut. Bull.* 123, 122-126.

1146 Lenz, R., Labrenz, M., 2018. Small microplastic sampling in water: Development of an encapsulated filtration device.
1147 *Water* 10, 1055.

1148 Lespes, G., Gigault, J., 2011. Hyphenated analytical techniques for multidimensional characterisation of submicron
1149 particles: A review. *Anal. Chim. Acta.* 692, 26-41.

1150 Li, P., Zou, X., Wang, X., Su, M., Chen, C., Sun, X., Zhang, H., 2020. A preliminary study of the interactions between
1151 microplastics and citrate-coated silver nanoparticles in aquatic environments. *J. Hazard. Mater.* 385, 121601.

1152 Li, S., Liu, H., Gao, R., Abdurahman, A., Dai, J., Zeng, F., 2018. Aggregation kinetics of microplastics in aquatic
1153 environment: Complex roles of electrolytes, pH, and natural organic matter. *Environ. Pollut.* 237, 126-132.

1154 Li, X., Logan, B.E., 2001. Permeability of fractal aggregates. *Water Res.* 35, 3373-3380.

1155 Li, Y., Wang, X., Fu, W., Xia, X., Liu, C., Min, J., Zhang, W., Crittenden, J.C., 2019. Interactions between nano/micro
1156 plastics and suspended sediment in water: Implications on aggregation and settling. *Water Res.* 161, 486-495.

1157 Liu, J., Zhang, T., Tian, L., Liu, X., Qi, Z., Ma, Y., Ji, R., Chen, W., 2019a. Aging significantly affects mobility and
1158 contaminant-mobilizing ability of nanoplastics in saturated loamy sand. *Environ. Sci. Technol.* 53, 5805-5815.

1159 Liu, L., Veerappan, V., Pu, Q., Cheng, C., Wang, X., Lu, L., Allen, R.D., Guo, G., 2013. High-resolution hydrodynamic
1160 chromatographic separation of large DNA using narrow, bare open capillaries: A rapid and economical alternative
1161 technology to pulsed-field gel electrophoresis? *Anal. Chem.* 86, 729-736.

1162 Liu, Y., Hu, Y., Yang, C., Chen, C., Huang, W., Dang, Z., 2019b. Aggregation kinetics of UV irradiated nanoplastics in
1163 aquatic environments. *Water Res.* 163, 114870.

1164 Long, M., Moriceau, B., Gallinari, M., Lambert, C., Huvet, A., Raffray, J., Soudant, P., 2015. Interactions between
1165 microplastics and phytoplankton aggregates: Impact on their respective fates. *Mar. Chem.* 175, 39-46.

1166 Long, M., Paul-Pont, I., Hegaret, H., Moriceau, B., Lambert, C., Huvet, A., Soudant, P., 2017. Interactions between
1167 polystyrene microplastics and marine phytoplankton lead to species-specific hetero-aggregation. *Environ. Pollut.* 228, 454-
1168 463.

1169 Mani, T., Hauk, A., Walter, U., Burkhardt-Holm, P., 2015. Microplastics profile along the Rhine River. *Sci. Rep-UK* 5,
1170 17988.

1171 Mao, Y., Ai, H., Chen, Y., Zhang, Z., Zeng, P., Kang, L., Li, W., Gu, W., He, Q., Li, H., 2018. Phytoplankton response to
1172 polystyrene microplastics: Perspective from an entire growth period. *Chemosphere* 208, 59-68.

1173 McCormick, A., Hoellein, T.J., Mason, S.A., Schlupe, J., Kelly, J.J., 2014. Microplastic is an abundant and distinct
1174 microbial habitat in an urban river. *Environ. Sci. Technol.* 48, 11863-11871.

1175 Meng, Z., Hashmi, S.M., Elimelech, M., 2013. Aggregation rate and fractal dimension of fullerene nanoparticles via
1176 simultaneous multiangle static and dynamic light scattering measurement. *J. Colloid Interf. Sci.* 392, 27-33.

1177 Messaud, F.A., Sanderson, R.D., Runyon, J.R., Otte, T., Pasch, H., Williams, S.K.R., 2009. An overview on field-flow
1178 fractionation techniques and their applications in the separation and characterization of polymers. *Prog. Polym. Sci.* 34,
1179 351-368.

1180 Mintenig, S.M., Bauerlein, P., Koelmans, A.A., Dekker, S.C., van Wezel, A., 2018. Closing the gap between small and
1181 smaller: Towards a framework to analyse nano- and microplastics in aqueous environmental samples. *Environ. Sci-Nano*
1182 5, 1640-1649.

1183 Montes Ruiz-Cabello, F.J., Trefalt, G., Oncsik, T., Szilagyi, I., Maroni, P., Borkovec, M., 2015. Interaction forces and
1184 aggregation rates of colloidal latex particles in the presence of monovalent counterions. *J. Phys. Chem. B* 119, 8184-8193.

1185 Murphy, F., Ewins, C., Carbonnier, F., Quinn, B., 2016. Wastewater treatment works (WwTW) as a source of microplastics
1186 in the aquatic environment. *Environ. Sci. Technol.* 50, 5800-5808.

1187 Nan, B., Su, L., Kellar, C., Craig, N.J., Keough, M.J., Pettigrove, V., 2020. Identification of microplastics in surface water
1188 and Australian freshwater shrimp *Paratya australiensis* in Victoria, Australia. *Environ. Pollut.* 259, 113865.

1189 Nguyen, B., Claveau-Mallet, D., Hernandez, L.M., Xu, E.G., Tufenkji, N., 2019. Separation and analysis of microplastics
1190 and nanoplastics in complex environmental samples. *Accounts Chem. Res.* 52, 858-866.

1191 Oberbeckmann, S., Loder, M.G.J., Labrenz, M., 2015. Marine microplastic-associated biofilms - A review. *Environ. Chem.*
1192 12, 551-562.

1193 Oriekhova, O., Stoll, S., 2018. Heteroaggregation of nanoplastic particles in the presence of inorganic colloids and natural
1194 organic matter. *Environ. Sci-Nano* 5, 792-799.

1195 Peeken, I., Primpke, S., Beyer, B., Gütermann, J., Katlein, C., Krumpfen, T., Bergmann, M., Hehemann, L., Gerdt, G.,
1196 2018. Arctic sea ice is an important temporal sink and means of transport for microplastic. *Nat. Commun.* 9, 1505.

1197 Philippe, A., Gangloff, M., Rakcheev, D., Schaumann, G., 2014. Evaluation of hydrodynamic chromatography coupled
1198 with inductively coupled plasma mass spectrometry detector for analysis of colloids in environmental media-effects of
1199 colloid composition, coating and shape. *Anal. Methods-UK* 6, 8722-8728.

1200 Pico, Y., Alfarhan, A., Barcelo, D., 2019. Nano- and microplastic analysis: Focus on their occurrence in freshwater
1201 ecosystems and remediation technologies. *TrAC-Trend. Anal. Chem.* 113, 409-425.

1202 Pico, Y., Barcelo, D., 2019. Analysis and prevention of microplastics pollution in water: Current perspectives and future
1203 directions. *ACS Omega* 4, 6709-6719.

1204 Pirok, B.W., Abdhussain, N., Aalbers, T., Wouters, B., Peters, R.A., Schoenmakers, P.J., 2017. Nanoparticle analysis by
1205 online comprehensive two-dimensional liquid chromatography combining hydrodynamic chromatography and size-

1206 exclusion chromatography with intermediate sample transformation. *Anal. Chem.* 89, 9167-9174.

1207 Praetorius, A., Badetti, E., Brunelli, A., Clavier, A., Gallego-Urrea, J.A., Gondikas, A., Hassellöv, M., Hofmann, T.,
1208 Mackevica, A., Marcomini, A., Peijnenburg, W., Quik, J.T.K., Seijo, M., Stoll, S., Tepe, N., Walch, H., von der Kammer,
1209 F., 2020. Strategies for determining heteroaggregation attachment efficiencies of engineered nanoparticles in aquatic
1210 environments. *Environ. Sci-Nano* 7, 351-367.

1211 Praetorius, A., Labille, J., Scheringer, M., Thill, A., Hungerbühler, K., Bottero, J.Y., 2014. Heteroaggregation of titanium
1212 dioxide nanoparticles with model natural colloids under environmentally relevant conditions. *Environ. Sci. Technol.* 48,
1213 10690-10698.

1214 Prata, J.C., da Costa, J.P., Duarte, A.C., Rocha-Santos, T., 2019. Methods for sampling and detection of microplastics in
1215 water and sediment: A critical review. *TrAC-Trend. Anal. Chem.* 110, 150-159.

1216 Qu, X., Hwang, Y.S., Alvarez, P.J.J., Bouchard, D., Li, Q., 2010. UV irradiation and humic acid mediate aggregation of
1217 aqueous fullerene (nC₆₀) nanoparticles. *Environ. Sci. Technol.* 44, 7821-7826.

1218 Quik, J., van De Meent, D., Koelmans, A., 2014. Simplifying modeling of nanoparticle aggregation-sedimentation
1219 behavior in environmental systems: A theoretical analysis. *Water Res.* 62, 193-201.

1220 Ramirez, L., Gentile, S.R., Zimmermann, S., 2016. Comparative study of the effect of aluminum chloride, sodium alginate
1221 and chitosan on the coagulation of polystyrene micro-plastic particles. *J. Colloid Sci. Biotechnol.* 5, 190-198.

1222 Revillon, A., 2000. Alternatives to size-exclusion chromatography. *J. Liq. Chromatogr.* 17, 2991-3023.

1223 Rezaei, M., Riksen, M., Sirjani, E., Sameni, A., Geissen, V., 2019. Wind erosion as a driver for transport of light density
1224 microplastics. *Sci. Total. Environ.* 669, 273-281.

1225 Romero-Cano, M.S., Martín-Rodríguez, A., de Las Nieves, F., 2000. Colloidal stabilization and destabilization of a
1226 carboxyl latex by adsorption of Triton X-100. *Macromol. Symp.* 151, 427-434.

1227 Romero-Cano, M.S., Martín-Rodríguez, A., de las Nieves, F.J., 2001. Electrosteric stabilization of polymer colloids with
1228 different functionality. *Langmuir* 17, 3505-3511.

1229 Ruiz-Cabello, F.J.M., Trefalt, G., Csendes, Z., Sinha, P., Oncsik, T., Szilagy, I., Maroni, P., Borkovec, M., 2013. Predicting
1230 aggregation rates of colloidal particles from direct force measurements. *J. Phys. Chem. B* 117, 11853-11862.

1231 Rummel, C.D., Jahnke, A., Gorokhova, E., Kühnel, D., Schmitt-Jansen, M., 2017. Impacts of biofilm formation on the fate
1232 and potential effects of microplastic in the aquatic environment. *Environmen. Sci. Tech. Let.* 4, 258-267.

1233 Runyon, J.R., Williams, S.K.R., 2011. Composition and molecular weight analysis of styrene-acrylic copolymers using
1234 thermal field-flow fractionation. *J. Chromatogr. A* 1218, 6774-6779.

1235 Saavedra, J., Stoll, S., Slaveykova, V.I., 2019. Influence of nanoplastic surface charge on eco-corona formation,
1236 aggregation and toxicity to freshwater zooplankton. *Environ. Pollut.* 252, 715-722.

1237 Schneider, C., Hanisch, M., Wedel, B., Jusufi, A., Ballauff, M., 2011. Experimental study of electrostatically stabilized
1238 colloidal particles: Colloidal stability and charge reversal. *J. Colloid Interf. Sci.* 358, 62-67.

1239 Schwaferts, C., Niessner, R., Elsner, M., Ivleva, N.P., 2019. Methods for the analysis of submicrometer- and nanoplastic
1240 particles in the environment. *TrAC-Trend. Anal. Chem.* 112, 52-65.

1241 Sendra, M., Staffieri, E., Yeste, M.P., Moreno-Garrido, I., Gatica, J.M., Corsi, I., Blasco, J., 2019. Are the primary
1242 characteristics of polystyrene nanoplastics responsible for toxicity and ad/absorption in the marine diatom *Phaeodactylum*
1243 *tricornutum*? *Environ. Pollut.* 249, 610-619.

1244 Shams, M., Alam, I., Chowdhury, I., 2020. Aggregation and stability of nanoscale plastics in aquatic environment. *Water*
1245 *Res.* 171, 115401.

1246 Shekunov, B.Y., Chattopadhyay, P., Tong, H.H.Y., Chow, A.H.L., 2006. Particle size analysis in pharmaceuticals: Principles,
1247 methods and applications. *Pharm. Res-Dordr* 24, 203-227.

1248 Shendruk, T.N., Slater, G.W., 2012. Operational-modes of field-flow fractionation in microfluidic channels. J. Chromatogr.
1249 A 1233, 100-108.

1250 Shendruk, T.N., Slater, G.W., 2014. Hydrodynamic chromatography and field flow fractionation in finite aspect ratio
1251 channels. J. Chromatogr. A 1339, 219-223.

1252 Shendruk, T.N., Tahvildari, R., Catafard, N.M., Andrzejewski, L., Gigault, C., Todd, A., Gagne-Dumais, L., Slater, G.W.,
1253 Godin, M., 2013. Field-flow fractionation and hydrodynamic chromatography on a microfluidic chip. Anal. Chem. 85,
1254 5981-5988.

1255 Silva, A.B., Bastos, A.S., Justino, C.I.L., da Costa, J.P., Duarte, A.C., Rocha-Santos, T.A.P., 2018. Microplastics in the
1256 environment: Challenges in analytical chemistry - A review. Anal. Chim. Acta. 1017, 1-19.

1257 Singh, N., Tiwari, E., Khandelwal, N., Darbha, G.K., 2019. Understanding the stability of nanoplastics in aqueous
1258 environments: Effect of ionic strength, temperature, dissolved organic matter, clay, and heavy metals. Environ. Sci-Nano
1259 6, 2968-2976.

1260 Skaf, D.W., Punzi, V.L., Rolle, J.T., Kleinberg, K.A., 2020. Removal of micron-sized microplastic particles from simulated
1261 drinking water via alum coagulation. Chem. Eng. J. 386, 123807.

1262 Song, Z., Yang, X., Chen, F., Zhao, F., Zhao, Y., Ruan, L., Wang, Y., Yang, Y., 2019. Fate and transport of nanoplastics in
1263 complex natural aquifer media: Effect of particle size and surface functionalization. Sci. Total Environ. 669, 120-128.

1264 Stawikowska, J., Livingston, A.G., 2013. Assessment of atomic force microscopy for characterisation of nanofiltration
1265 membranes. J. Membrane. Sci. 425, 58-70.

1266 Stock, F., Kochleus, C., Bänsch-Baltruschat, B., Brennholt, N., Reifferscheid, G., 2019. Sampling techniques and
1267 preparation methods for microplastic analyses in the aquatic environment - A review. TrAC-Trend. Anal. Chem. 113, 84-
1268 92.

1269 Suhrhoff, T.J., Scholz-Böttcher, B.M., 2016. Qualitative impact of salinity, UV radiation and turbulence on leaching of
1270 organic plastic additives from four common plastics - A lab experiment. Mar. Pollut. Bull. 102, 84-94.

1271 Summers, S., Henry, T., Gutierrez, T., 2018. Agglomeration of nano- and microplastic particles in seawater by
1272 autochthonous and de novo-produced sources of exopolymeric substances. Mar. Pollut. Bull. 130, 258-267.

1273 Sun, J., Dai, X., Wang, Q., van Loosdrecht, M.C.M., Ni, B.-J., 2019. Microplastics in wastewater treatment plants:
1274 Detection, occurrence and removal. Water Res. 152, 21-37.

1275 Sun, X., Chen, B., Li, Q., Liu, N., Xia, B., Zhu, L., Qu, K., 2018. Toxicities of polystyrene nano- and microplastics toward
1276 marine bacterium *Halomonas alkaliphila*. Sci. Total Environ. 642, 1378-1385.

1277 Tallec, K., Blard, O., Gonzalez-Fernandez, C., Brotons, G., Berchel, M., Soudant, P., Huvet, A., Paul-Pont, I., 2019. Surface
1278 functionalization determines behavior of nanoplastic solutions in model aquatic environments. Chemosphere 225, 639-
1279 646.

1280 Thiagarajan, V., Iswarya, V., Seenivasan, R., Chandrasekaran, N., Mukherjee, A., 2019. Influence of differently
1281 functionalized polystyrene microplastics on the toxic effects of P25 TiO₂ NPs towards marine algae *Chlorella* sp. Aquat.
1282 Toxicol. 207, 208-216.

1283 Trefalt, G., Palberg, T., Borkovec, M., 2017. Forces between colloidal particles in aqueous solutions containing monovalent
1284 and multivalent ions. Curr. Opin. Colloid In. 27, 9-17.

1285 United States Congress (2015) H.R.1321 - Microbead-Free Waters Act of 2015.

1286 Viršek, M.K., Lovšin, M.N., Koren, Š., Kržan, A., Peterlin, M., 2017. Microplastics as a vector for the transport of the
1287 bacterial fish pathogen species *Aeromonas salmonicida*. Mar. Pollut. Bull. 125, 301-309.

1288 Wagner, T., Lipinski, H.-G., Wiemann, M., 2014. Dark field nanoparticle tracking analysis for size characterization of
1289 plasmonic and non-plasmonic particles. J. Nanopart. Res. 16, 2419.

1290 Wang, H., Adeleye, A.S., Huang, Y., Li, F., Keller, A.A., 2015. Heteroaggregation of nanoparticles with biocolloids and
1291 geocolloids. *Adv. Colloid Interfac.* 226, 24-36.

1292 Wang, J., Zhao, X., Wu, A., Tang, Z., Niu, L., Wu, F., Wang, F., Zhao, T., Fu, Z., 2020. Aggregation and stability of sulfate-
1293 modified polystyrene nanoplastics in synthetic and natural waters. *Environ. Pollut.*,
1294 <https://doi.org/10.1016/j.envpol.2020.114240>.

1295 Wang, W., Wang, J., 2018. Investigation of microplastics in aquatic environments: An overview of the methods used, from
1296 field sampling to laboratory analysis. *TrAC-Trend. Anal. Chem.* 108, 195-202.

1297 Ward, J.E., Kach, D.J., 2009. Marine aggregates facilitate ingestion of nanoparticles by suspension-feeding bivalves. *Mar.*
1298 *Environ. Res.* 68, 137-142.

1299 Wu, J., Jiang, R., Lin, W., Ouyang, G., 2019a. Effect of salinity and humic acid on the aggregation and toxicity of
1300 polystyrene nanoplastics with different functional groups and charges. *Environ. Pollut.* 245, 836-843.

1301 Wu, P., Huang, J., Zheng, Y., Yang, Y., Zhang, Y., He, F., Chen, H., Quan, G., Yan, J., Li, T., Gao, B., 2019b. Environmental
1302 occurrences, fate, and impacts of microplastics. *Ecotox. Environ. Safe.* 184, 109612.

1303 Xanthos, D., Walker, T.R., 2017. International policies to reduce plastic marine pollution from single-use plastics (plastic
1304 bags and microbeads): A review. *Mar. Pollut. Bull.* 118, 17-26.

1305 Xiao, Y., Tan, Z., Yin, Y., Guo, X., Xu, J., Wang, B., Fan, H., Liu, J., 2018. Application of hollow fiber flow field-flow
1306 fractionation with UV-Vis detection in the rapid characterization and preparation of poly (vinyl acetate) nanoemulsions.
1307 *Microchem. J.* 137, 376-380.

1308 Xu, Z., Xiong, X., Zhao, Y., Xiang, W., Wu, C., 2020. Pollutants delivered every day: Phthalates in plastic express
1309 packaging bags and their leaching potential. *J. Hazard. Mater.* 384, 121282.

1310 Yang, J., Xu, L., Lu, A., Luo, W., Li, J., Chen, W., 2018. Progress in the source and toxicology of micro (nano) plastics in
1311 the environment. *Environ. Chem.* 37, 383-396.

1312 Yu, S., Shen, M., Li, S., Fu, Y., Zhang, D., Liu, H., Liu, J., 2019. Aggregation kinetics of different surface-modified
1313 polystyrene nanoparticles in monovalent and divalent electrolytes. *Environ. Pollut.* 255, 113302.

1314 Zhang, C., Chen, X., Wang, J., Tan, L., 2017. Toxic effects of microplastic on marine microalgae *Skeletonema costatum*:
1315 Interactions between microplastic and algae. *Environ. Pollut.* 220, 1282-1288.

1316 Zhang, C., Wang, C., Cao, G., Wang, D., Ho, S.-H., 2020. A sustainable solution to plastics pollution: An eco-friendly
1317 bioplastic film production from high-salt contained *Spirulina* sp. residues. *J. Hazard. Mater.* 388, 121773.

1318 Zhang, W. 2014. Nanoparticle Aggregation: Principles and Modeling. *Nanomaterial: Impacts on Cell Biology and*
1319 *Medicine.* Springer, pp. 19-43.

1320 Zhang, Z., Chen, Y., 2019. Effects of microplastics on wastewater and sewage sludge treatment and their removal: A review.
1321 *Chem. Eng. J.* 382, 122955.

1322 Zhao, S., Ward, J.E., Danley, M., Mincer, T.J., 2018. Field-based evidence for microplastic in marine aggregates and
1323 mussels: Implications for trophic transfer. *Environ. Sci. Technol.* 52, 11038-11048.

1324 Zhu, Z., Wang, S., Zhao, F., Wang, S., Liu, F., Liu, G., 2019. Joint toxicity of microplastics with triclosan to marine
1325 microalgae *Skeletonema costatum*. *Environ. Pollut.* 246, 509-517.

1326 Zobkov, M.B., Esiukova, E.E., 2018. Microplastics in a marine environment: Review of methods for sampling, processing,
1327 and analyzing microplastics in water, bottom sediments, and coastal deposits. *Oceanology* 58, 137-143.

1328